

The Arctic reality versus NASA's MODIS Satellites: An overview of the Kevo Valley terrain, Finland



733160

BSc (Hons) Geography

2017

Supervisor: Dr Nicholas Pepin

Word Count: 9892



UNIVERSITY of PORTSMOUTH

Declaration

I, the undersigned, declare that this Independent Study is exclusively my own work (except where the work of others is acknowledged). I give permission for this work to be photocopied, archived and made available for inter-library loan. Ethical issues associated with the research have been considered and appropriate procedures adhered to.

Signed.....

Dated.....

Acknowledgements

I would like to firstly thank Dr. Nick Pepin for his support and guidance since joining the university and throughout my time as one of his tutees. Without of which I would not have had the experience to conduct ‘once in a life time’ field work in an area of such natural beauty, and experience phenomena such as the Aurora Borealis. I would also like to thank Martin Schaefer and Linley Hastewell. Martin, for his support throughout the fieldwork week, and continued support with my GIS ideas and conundrums. Linley for providing the field equipment for the weeks study and also the equipment information allowing for accurate analysis.

There are three people of which I owe a lot of gratitude for their continued support across the study trip week, one of which being Luke Mitchell. Luke offered his support and dedicated his time across the study week by travelling to nearly all the 65 sites with myself, Nick and Martin. Where he collected many of my results and carried much of the equipment. The last two people I would like to thank for their support during this week, is Spencer Read and Tom Singleton. While also being my dear friends they offered invaluable support with both data collection, analysing and great company throughout the week and the subsequent weeks spent in the library. Thanks also goes to the staff at the Kevo Subarctic Research Institute, for there hospitality and information upon the local environment and culture.

Lastly, I would like to thank my friends and my family for the continued care and encouragement throughout this period. Providing both love, advice and bucket loads of coffee.

Contents

Declaration	I
Acknowledgements	II
List of Abbreviations.....	V
List of Figures	VI
List of Maps	VII
List of Tables.....	VIII
Abstract	IX
Chapter 1: Introduction.....	1
1.0 Introductory review	2
1.1 The recent changing climate of the Arctic Circle.....	2
1.2 Snow characteristics and topography	3
1.3 Use of GIS and remote sensing	4
1.4 Accuracy of MODIS imagery	6
1.5 Study area	8
1.6 Aims and objectives	10
Chapter 2: Methods	11
2.0 Methodology	12
2.1 Field data	12
2.2 Secondary data.....	13
2.2.1 Secondary data sourcing.....	14
2.2.2 Secondary data elements	15
2.3 Data analysis.....	15
2.3.1 Heat map analysis.....	15
2.3.2 Terrain analysis	15
2.4 Radiation analysis.....	16
2.5 Satellite data analysis	17
2.5.1 Cloud cover calculation.....	17
Chapter 3: Results	18
3.0 Results	20
3.1 Elevation.....	20
3.2 Snow depth.....	20
3.3 Snow density	23
3.4 Surface radiation	23
3.5 Snowpack surface temperature.....	26

3.6 Snowpack base temperature	26
3.7 Aspect.....	29
3.8 Curvature	29
3.9 Albedo	29
Chapter 4: Analysis.....	32
4.0 Satellite analysis and interpretation.....	33
4.1 Satellite spatial and temporal coverage.....	33
4.2 Terra, Aqua and field data comparisons.....	35
4.2.1 Surface reflectance	36
4.2.2 Land surface temperature	37
4.3 Albedo vs MOD09	38
4.3.1 Albedo analysis and further interpretation	39
4.4 Surface temperature vs MOD11	42
4.4.1 LST analysis and further interpretation.....	43
4.5 Principal Components Analysis	44
4.5.1 Principal Component Analysis for non-MODIS variables (PCA1).....	45
4.5.2 Principal components analysis for all variables (PCA2).....	46
4.6 Summary of analysis	47
Chapter 5: Discussion	48
5.0 Discussion	49
5.1 Synoptic conditions: Resultant radiative forcing	49
5.2 MODIS representation of cloud cover	50
5.3 The compromise between field data and satellite data.....	51
Chapter 6: Conclusion	52
6.0 Conclusion.....	53
6.1 Critical reflection.....	53
6.2 Further research.....	54
Chapter 7: References.....	56
7.0 References	57
Chapter 8: Appendices.....	63
8.0 Appendices	64

List of Abbreviations

MODIS – Moderate Resolution Imagine Spectro-Radiometer

GIS – Geographical Information System

MYD – Aqua product

MOD – Terra product

NASA – National Aeronautics and Space Administration

NSIDC – National Snow and Ice Data Center.

LST – Land Surface Temperature

SREF – Surface Reflectance

EOS – Earth Observatory System

AIRS – Atmospheric Infrared Sounder

ASTER – Advanced Spaceborne Thermal Emission and Reflection Radiometer

CERES – Clouds and the Earth's Radiant Energy System

MISR – Multi-angle Imaging SpectroRadiometer

MOPITT – Measurement of Pollution in the Troposphere

AMSR/E – Advanced Microwave Scanning Radiometer for EOS

AMSU – Advanced Microwave Sounding Unit

HSB – Humidity Sounder for Brazil

CMG – Climate Modelling Grid

HDF4 – Hierarchical Data Format 4

H##V## – Tile co-ordinates for satellite data retrieval where H## is number of the horizontal tile and V## is the number of the vertical tile.

DEM – Digital Elevation Model

DSA – Daily Satellite Albedo

CSA – Composite Satellite Albedo

DST – Daily Satellite Temperature

CST – Composite Satellite Temperature

MST – Manual Satellite Temperature

PCA – Principle Component Analysis

PC – Principle Component

IPCC – Intergovernmental Panel on Climate Change

List of Figures

Figure 1: Diagram of multiple interlinking feedback loops at play within the Arctic system. The arrows indicate positive forcing unless otherwise stated with a minus sign. (Chapin et al, 2005).....	2
Figure 2: Flow diagram adapted from www.snobear.colorado.edu (Williams, 2004).....	3
Figure 3: Sketch of Terra satellite, from the NASA's EOS. Retrieved from NASA (2015).....	5
Figure 4: The order summary for MOD11A2. The same process was undertaken for all MODIS datasets: MOD11A1, MYD11A1, MOD11A2, MYD11A2, MOD09GQ, MYD09GQ, MOD09G1 and MYD09G1. Retrieved from 'DAAC2Disk LP DAAC :: NASA Land Data Products and Services' (2014).....	14
Figure 5: Two differing curvature outputs: planform and profile. Retrieved from 'Curvature function' (2016).....	16
Figure 6: General curvature analysis output. Retrieved from Jenness (2007, p.13)	16
Figure 7: Synoptic chart for day 70 (Thursday 10th March) in comparison to MOD09GQ imagery, with day 66 on the left and day 70 on the right. Retrieved from www.willandweather.org.uk/mycharts.php (2016), Vermote, E. (2015a).....	40
Figure 8: Principal Component Analysis for all non-MODIS variables. Full PCA in appendix F.1.....	45
Figure 9: Principal Component Analysis for all MODIS variables. Full PCA in appendix F.2.	46
Figure 10: Synoptic charts comparing weather between 6 th March (Day 66 – left) and 10 th March (Day 70 – right). Retrieved from www.willandweather.org.uk/mycharts.php (2016).	49
Figure 11: SI-121 in the field, photo of clear site experiment. Retrieved from Pepin (2017).	54
Figure 12: Correlation coefficients for both the overall dataset and the site specific data sets. Data provided by Pepin (2017).	55

List of Maps

Map 1: Stereographic polar projection showing research site, Arctic Circle, July 10° isotherm and tree line. Data has been retrieved from ArcGIS Online via “Arctic Ocean Base” (2015), “Tree Line” (2015).....	9
Map 2: Elevation for each measured point across the study area. The map shows both elevation and point name for locational reference.	19
Map 3: Heat map of snow depth for each measured point.	21
Map 4: Heat map of snow density for each measured point.	22
Map 5: Heat map of solar radiation both incoming and outgoing, for the study area.....	24
Map 6: Isotherm map for temperature at the top of the snowpack.	25
Map 7: Isotherm map for temperature at the bottom of the snowpack.	27
Map 8: Terrain analysis: Aspect.....	28
Map 9: Terrain Analysis: Curvature.....	30
Map 10: Manual Albedo heat map for study area.	31
Map 11: Comparison of MOD11 coverage for both daily and composite sensor data.	34
Map 12: Visualisation of MODIS Terra albedo comparison to manual albedo data.	38
Map 13: Visualisation of MODIS Terra LST comparison to manual SST data. Daily data is used within a day 70 micro study.....	42

List of Tables

Table 1: MODIS Spectral Bands where dataset band number is listed with its primary use, bandwidth and resolution. Retrieved from Lillesand et al (2014, p.374).....	6
Table 2: Overview of field methods.....	12
Table 3: All MODIS subsets used for the eight separate datasets. Retrieved from lpdaac.usgs.gov (2014).....	15
Table 4: Cloud cover percentage for okta value throughout the study week.....	33
Table 5: Correlation Matrix for all variables.	35
Table 6: P value table showing the significance of statistical difference between SREF satellites and products.	36
Table 7: P value table showing the significance of statistical difference between LST satellites.....	37
Table 8: Albedo correlation coefficients for manual vs satellite datasets.....	39
Table 9: PUKS transect albedo vs elevation analysis.	41
Table 10: LST correlation coefficients for manual vs satellite datasets.	43
Table 11: Data table for SI-121 sensor vs MOD11A1, 2017 study. Data provided by Pepin (2017).	54

Abstract

Satellite measurements are used within academia, as a proxy for ground data across inaccessible areas of the globe, or where in situ is sparse. The expectation of these datasets is to provide an accurate representation of ground variables, however this may not be the case, particularly for Arctic regions. A large spatial study was undertaken to collect appropriate ground variables across the Kevo Valley, Finland. Field data included the measurement of 6 variables for 65 points, within 40 km². A comparison of MODIS Terra and Aqua resulted in primary use of Terra as a secondary dataset. Both surface temperature and albedo values were extracted for the points and compared across both daily and composite MODIS Terra datasets, where disparities between the composite rasters are larger than that of the available daily rasters. The implications were therefore the availability of clear sky data, and how cloud contamination effected the representation of valley processes such as cloud radiative forcing and changing ground albedo. Concluding statements find that satellite datasets, while being an essential part of climatic data, must be approached with a degree of scepticism, where the ability to compare to ground control sites is vital.

Chapter 1:

Introduction

1.0 Introductory review

1.1 The recent changing climate of the Arctic Circle

Geographically, researchers agree that the Arctic Circle is the area above 66.5°N (Serreze & Barry, 2009, p.17). Above this latitude a change in solar geometry becomes evident with the result of 24-hour days of darkness and daylight in the winter and summer, respectively. This characteristic of the Arctic is called the polar night and the polar day. With respect to climate change, the Arctic is said to be undergoing an amplification of surface warming by approximately double that of global recorded averages (ACIA, 2005; IPCC, 2007).

As a result of these past records, the Arctic is a priority of study to understand the Earth's relationship with a changing climate. Features of the Arctic system that are changing include sea ice, snow, snowline, treeline and cold temperatures (Serreze & Barry, 2009, pp.37–54). These characteristics are often referred to as feedback processes that magnify or diminish the radiative influence due to warming or cooling (Cubasch & Cess, 1990). In particular sea ice - albedo feedback is the positive loop of warming induced sea

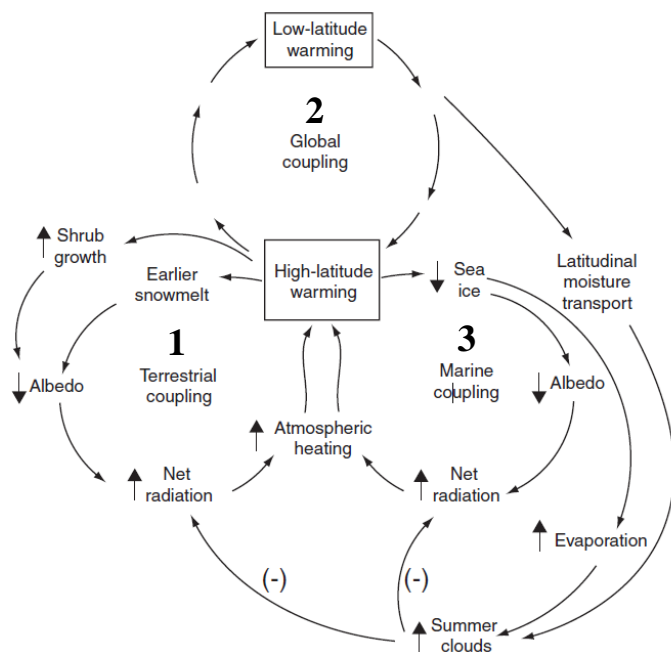


Figure 1: Diagram of multiple interlinking feedback loops at play within the Arctic system. The arrows indicate positive forcing unless otherwise stated with a minus sign. (Chapin et al, 2005)

ice decline further decreasing the overall albedo of sea ice extent and resulting in decreased radiation reflectance and further warming. Cohen et al (2014) recorded such sea ice decline in the month of September at 12.4% per decade since 1979.

While this is evidence of one Arctic characteristic changing with surface warming amplification, Cohen et al (2014) go on to state that snow cover—a key Arctic climate feature—has seen a decrease in the month of June by a factor of 2 to that of sea ice decrease. This combined loss of two Arctic climate features, which diminish the Arctic winter season and thus increase the autumnal and spring seasons, are a direct result of accelerated surface warming (Chapin et al, 1992, p.11).

The snowline, as an Arctic feature, is affected by changing elevation and changing latitude (Serreze & Barry, 2009, p.51). The snowline is anticipated to retreat with a warming Arctic climate (Pepin et al, 2015, p.425). Furthermore, the rate of change for the snowline retreat may increase with the rising temperatures (Hantel et al, 2000). The snowline variability is dictated by snowpack longevity, as described by Saunders et al (2008), and is likely to decrease in the winter and spring seasons with warming. This shift in hydrological balance will manifest in accumulation and the movement of the snowline upwards, reducing net albedo of mountains. This positive feedback loop only acts to accelerate snow loss.

1.2 Snow characteristics and topography

This complex and fickle form of precipitation is a key pillar of an Arctic environment. The properties of fallen snowpack generally include the temperature of top and bottom of the snow, and the resultant difference of both highlights the snowpack insolation characteristics. Albedo, or the reflectance of the snow surface, is controlled by impurities, while the water equivalent and liquid water content are both controlled by the characteristics in Figure 2 (Williams, 2004).

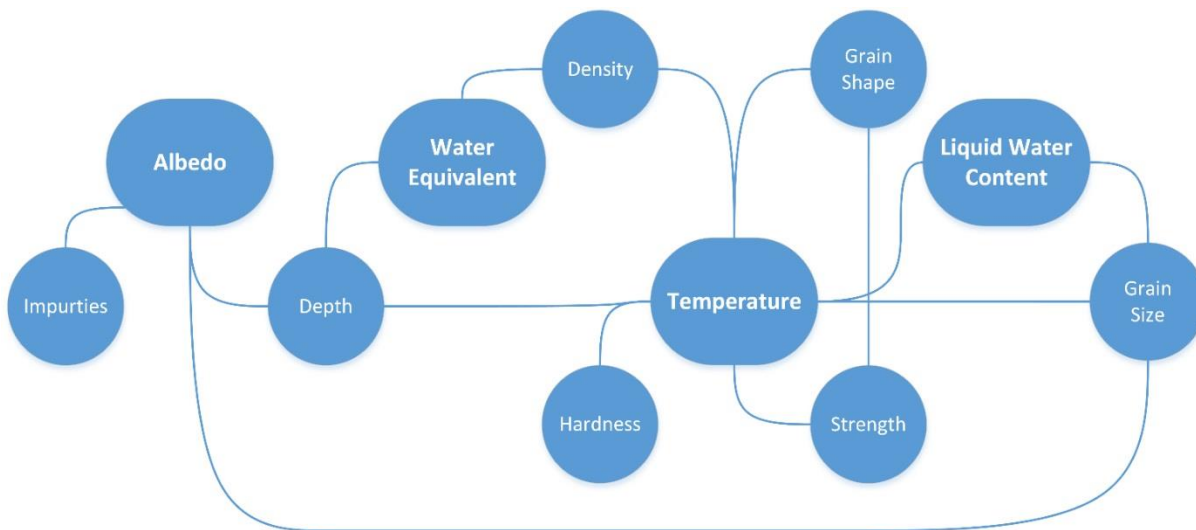


Figure 2: Flow diagram adapted from www.snowbear.colorado.edu (Williams, 2004).

Figure 2 recognises the complexity of the Arctic element, snow. While these snow properties and characteristics define the snowpack, the greater atmospheric controls are weather events bringing the snow, the frequency of the weather events, the conditions between snowfall events, and the topography and vegetation cover on which the snow accumulates (Rasmus, 2005, p.15). The final snow cover can be summarised as a combination of post-fall factors: accumulation and ablation.

Accumulation can be defined as the amount of snow deposited upon a surface from either one or many atmospheric events and processes. *Ablation* is defined as the process by which snow or ice is lost from a surface; via melting, evaporation, sublimation and Aeolian forcing (Thomas & Goudie, 2000). These processes interlink heavily with the snowpack's landscape topography. Slope and aspect are important topographic features and, according to McKay and Gray (1981), are important to snow distribution. They describe how slope direction inline of prevailing winds show shallow snow depths; this is also common on hill-tops. However, areas in the lee of slopes and gully formation see large amounts of accumulation; these hilltop and gully formations control snow accumulation due to slope curvature. While slope and curvature are key to accumulation and Aeolian ablation, certain aspects of the ground affect the energy budget between the sun and the surface snowpack (Rasmus, 2005, p.17).

Studies, such as Donald et al (1995), derive a snow cover coefficient of variation that can classify differing ground types, such as forest or lawn. The larger the coefficient, the larger the variability, which results in differing ablation rates across an area and differing snow melt patterns (Rasmus, 2005, p.16). This study shows a real quantification for snow cover and can begin to describe the topographic impact on snow processes.

1.3 Use of GIS and remote sensing

A *Geographical Information System* (GIS) describes a computer application with the ability to analyse location, patterns, trends and conditions (Heyward et al, 2011, p.3). However, a consensus is that GIS is a computer system that can hold, use and manipulate data of the Earth's surface (Rhind, 1989). The main components of GIS are, the system, spatial data and analysis tasks (Heyward et al, 2011, p.18). Remote sensing is fully integrated within GIS (Indiana University, 2015). This is the process of acquiring data of a surface/object through a device not in contact with the point of interest (Lillesand et al, 2014, p.1). Often the most important sensor is the eye and how it acquires the data. Commonly, aircrafts and satellites execute remote sensing, allowing the ability to consign to a 'science of observation from a distance' (Barrett & Curtis, 1999, p.6).

Since the development of high-resolution satellite data, such as Landsat and thematic mapper, the availability of satellite data to the user has increased (Barrett & Curtis, 1999, p.12). These satellites record electromagnetic radiation, which is characterised by wave frequency and wavelength, and commonly the use of the ultraviolet, visible, infrared and microwave light spectrums is paramount (Campbell & Wynne, 2011). This radiation recorded by the satellite is

then split into deferring bands or categories to give raster files with pixel values for an area and scale (Williams, 1995, p.96). These pixel values equate to a particular data attribute, such as land surface temperature. Satellites often carry multiple remote sensing equipment, with one such example being an ‘Earth Observation System’ (EOS) as devised by NASA. Terra and Aqua are of interest for this study and are ‘flagship’ EOS launched in 1999 and 2002, respectively (Lillesand et al, 2014, p.371).

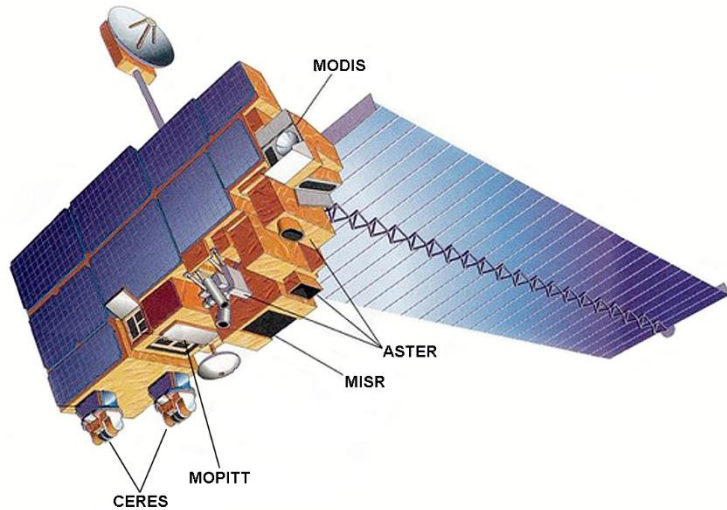


Figure 3: Sketch of Terra satellite, from the NASA's EOS. Retrieved from NASA (2015).

While Terra has five instruments—ASTER, CERES, MISR, MODIS and MOPITT (Figure 3)—the sister satellite Aqua has six instruments—MODIS, CERES, AMSR/E, AMSU, AIRS and HSB (Lillesand et al, 2014, p.372). These twin satellites are of a near-polar orbit, which is sun-synchronous of an altitude of 705 km (Lillesand et al, 2014, p.373).

The reason for these twin satellites is to enable cloud free data records (National Snow and Ice Data Center, n.d.; Lillesand et al, 2014, p.373), with Terra descending the equator at 10:30 and Aqua ascending at 13:30.

1.4 Accuracy of MODIS imagery

As stated above, the Moderate Resolution Imagine Spectro-Radiometer (MODIS) is stationed on NASA's Terra and Aqua EOS satellites. This sensor is expected to collect data of Earth's atmosphere, land and oceans (Lillesand et al, 2014, p.373). As explained by Campbell and Wynne (2011), these earth components are recorded as bands of wavelength. Table 1 shows all bands recognised by MODIS and their resultant properties.

MODIS Spectral Bands

Primary Use	Band	Bandwidth	Resolution (m)
Land/cloud boundaries	1	620–670 nm	250
	2	841–876 nm	250
Land/cloud properties	3	459–479 nm	500
	4	545–565 nm	500
	5	1230–1250 nm	500
	6	1628–1652 nm	500
	7	2105–2155 nm	500
Ocean color/phytoplankton/biogeochemistry	8	405–420 nm	1000
	9	438–448 nm	1000
	10	483–493 nm	1000
	11	526–536 nm	1000
	12	546–556 nm	1000
	13	662–672 nm	1000
	14	673–683 nm	1000
	15	743–753 nm	1000
	16	862–877 nm	1000
Atmospheric water vapor	17	890–920 nm	1000
	18	931–941 nm	1000
	19	915–965 nm	1000
Surface/cloud temperature	20	3.660–3.840 μm	1000
	21 ^a	3.929–3.989 μm	1000
	22	3.929–3.989 μm	1000
	23	4.020–4.080 μm	1000
Atmospheric temperature	24	4.433–4.498 μm	1000
	25	4.482–4.549 μm	1000
Cirrus clouds	26 ^b	1.360–1.390 μm	1000
Water vapor	27	6.538–6.895 μm	1000
	28	7.175–7.475 μm	1000
	29	8.400–8.700 μm	1000
Ozone	30	9.580–9.880 μm	1000
Surface/cloud temperature	31	10.780–11.280 μm	1000
	32	11.770–12.270 μm	1000
Cloud top altitude	33	13.185–13.485 μm	1000
	34	13.485–13.758 μm	1000
	35	13.785–14.085 μm	1000
	36	14.085–14.385 μm	1000

Table 1: MODIS Spectral Bands where dataset band number is listed with its primary use, bandwidth and resolution. Retrieved from Lillesand et al (2014, p.374)

Lillesand et al (2014, p.373) state calibration percentages for these MODIS bands where the accuracy of the 20 solar bands is 5% or more and the 16 thermal bands is 1% or more. Morain and Budge (2004, p.111) and Thome et al (2003) corroborate these values. Such strict calibration boundaries are necessary for long-term observations, such as those produced by Terra and Aqua. Lastly, MODIS swath is $\pm 55^\circ$ which covers a 2330 km width of the Earth's surface (Lillesand et al, 2014, p.373). As first suggested by Foody and Atkinson (2002, p.136), reflectance and emissivity data can be expected to improve with the development of sensors, such as MODIS; however, initial calibration assessed by Thome et al (2003) confirm inaccuracies between Terra and Aqua prior to 2002 with those uncertainties lingering into reflection calibration post-2002. This brings into question the accuracy of MODIS products from all its sensors within the present-day datasets.

Uncertainty among academics regarding MODIS products is known; however, bias within data use is unclear, with studies suggesting precision (Vermote et al, 2002; Wolfe et al, 2002; Wan et al, 2004; Zhao et al, 2005) and imprecision (Hall & Riggs, 2007; Lunetta et al, 2006; Stroeve et al, 2005; Zhao et al, 2006). It is, however, necessary to consider the history and accuracy of the MODIS sensor sets in question for this study. The two forms of Terra and Aqua MODIS products of interest for this study are Land Surface Temperature (LST) characterised by MOD11 by Terra and MYD11 by Aqua (Wan et al, 2015). There is also, surface reflectance (SREF) characterised by MOD09 by Terra and MYD09 by Aqua (Vermote, 2015). Since release there have been two versions of MOD11: C4 and C5. According to the MODIS Land Surface Temperature Products Users' Guide (Wan, 2006) updates were made from C4 to C5 (also known as V4 to V5) since 2006.

The consequences of these updates are specific to MOD11 products; and the study included MOD11A1 and its 8-day composite, MOD11A2. The MOD11A1 data set is a sinusoidal projection and a pixel boundary average of MOD11_L2 results, where MOD11_L2 LST product is generated by the according algorithm (Wan, 1999) of three rules that pixels must fall within:

1. Have nominal Level 1B radiance data in bands 31 and 32,
2. Are on land or inland water,
3. Are in clear-sky conditions at a confidence defined by MOD35
($>=95\%$ over land $<= 2000\text{m}$ or $>= 66\%$ over land $> 2000\text{m}$,
and at a confidence of $>= 66\%$ over lakes).

(Wan, 2006)

Furthermore, Wan (2006) mentioned how ‘A large uncertainty may exist in such estimated emissivity’s in semi-arid and arid areas’ within MOD11_L2, from which MOD11A2 composite is a secondary derivative. In addition, across the updates from C4 to C5, Wan (2006) illustrates in his table from Appendix A, that MOD11A1 data—the first derivative of MOD11_L2—is no longer based on temporal averaging (Line 2), and the removal of cloud contamination is now practiced in LST algorithms (Line 8). While it can be expected that this update was to reduce error within LST data for MOD11, further comparison of data to that of AIRs and ASTER LST products situated on either Terra or Aqua EOS, shows this is not the case—so much so, that ‘Products indicate that the land surface temperature in the C5 CMG products underestimated LST by up to 6K in some desert regions’ (NASA, 2016).

Further updates have not undergone such comparisons; thus, this study aims to assess in situ data alongside MOD11A1 and MOD11A2 LST 1 km resolution product to see any parallel with in situ recordings or any effect from past known issues for updated and current products. There will be an assessment of MOD09GQ and MOD09Q1 Surface Reflectance 250m resolution product. While there is no evidence of an undependable past, the likes of that seen within MOD11 LST products, it will be interesting to see how this climatic component of snowpack property is represented by the MODIS ‘eye in the sky’.

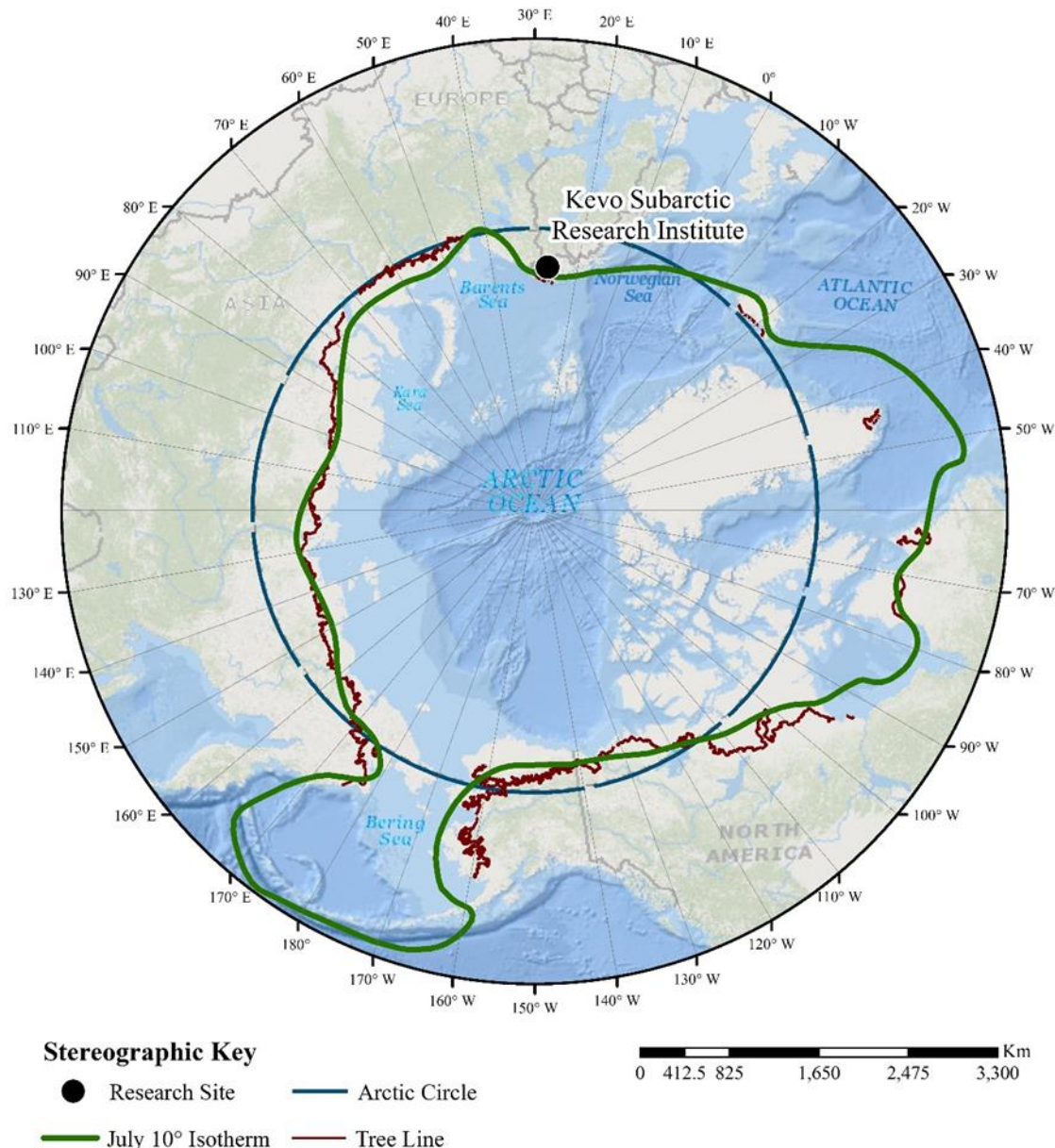
1.5 Study area

Kevo Subarctic Research Station is located in Utsjoki at the northernmost tip of Finland, 100 km from the coast of the Arctic Ocean. It lies about 60 km north of the continuous pine forest line (Eu-interact.org, 2016). The site co-ordinates are 69°45' N, 27°01' E.

Snowpack in Kevo begins to form from the beginning of the winter, up until March where it reaches an average depth of around 60 cm. This month was chosen to show the biggest variations in snow properties per site. The change in snowpack properties will be researched and recorded during the first week of the field trip in 2016.

Map 1 is a stereographic, azimuthal projection of the Arctic Circle. This map brings an understanding of broad climate forced over the Arctic. While the Arctic Circle is a defined cartographic line, the most northerly of the five major latitudes and the ‘latitude at which the sun does not rise in mid-winter or set in mid-summer (Goudie, & Thomas, 2000, p.28), the treeline and the 10°C isotherm line are climatic features that are ever changing. The green 10°C

July isotherm line describes the temperature boundary where temperatures inside this feature never exceed 10°C in the major summer month of the year, July; whereas the maroon treeline shows the extent of tree growth towards the pole where past this no vegetation can survive.



Map 1: Stereographic polar projection showing research site, Arctic Circle, July 10° isotherm and tree line. Data has been retrieved from ArcGIS Online via “Arctic Ocean Base” (2015), “Tree Line” (2015).

The concern with both Arctic climatic definitions is that they will become ever smaller with a rising polar climate (Grace, 2002), until the pole is no longer considered Arctic in temperature, and vegetation vacancy.

1.6 Aims and objectives

The overall aim of the project is to directly compare elements of manually recorded processes within the Arctic against MOD11 and MOD09 MODIS datasets, with two sub aims:

- Spatial and statistical representation of the relationships between all grounds-measured variables, alongside chosen satellite counterparts.
- Two focused studies upon MOD11, MOD09, and their appropriate manual counterparts with further interest upon reasoning for any discrepancies found.

Objectives include:

- Spatial representation of all manual data.
- Consideration of discrepancies between MODIS Aqua/Terra and Daily/Composite data.
- A full outline of influences upon MODIS and manual differences, including further discussion of satellite usage in current studies.
- The proposal of further study within this field, using newer and better-suited manual equipment and satellite datasets.

Chapter 2:

Methods

2.0 Methodology

2.1 Field data

Data collection took place from 5 March to 13 March 2016, where 65 locations were visited and measured.

The equipment used was as follows:

- Temperature probe (manual & electronic)
- Solarimeter
- Yardstick
- Tape measure
- Small snow wedge
- Scales
- Compass
- Walking pole (for electronic temperature probe)

Kevo sub-arctic research institute was the centre for research. A route transect was planned for each day that covered 7 to 10 points. Each point was signified by a Stevenson's screen. At each site it was necessary to dig a small surface snow pit at 20 cm from the surface. From there the four invasive and two passive measurements were taken, as shown in table 2.

Type	Variable	Process
Invasive	Surface snowpack temperature	A manual temperature probe was inserted just below the surface of the snow.
Invasive	Base snowpack temperature	A digital temperature probe, attached to an extendable walking pole, was driven into the snowpack close to the point to give an isolated reading.
Invasive	Snowpack weight and density	A small snow wedge of volume 250 g was used appropriately to preserve snowpack compression. Weighed in the field using scales.
Invasive	Depth	A yardstick was used to measure snow depth at the point, within a 1 m radius, both cardinally and ordinally.
Passive	Albedo	The count on the dial was recorded for 30 seconds for incoming solar radiation and outgoing solar reflectance. The sensor was held at 20 cm from the surface.
Passive	Vegetation	The vegetation count split was into size and type for a 10 m radius. Vegetation types include Birch, Pine and Aspin categorised as shrub, medium and big.

Table 2: Overview of field methods.

2.2 Secondary data

Jones (2009) defines secondary data as data collected by different researchers than those undertaking the analysis.' This provides a wider scope of comparison with new variables that otherwise wouldn't have been available via primary means. Often these secondary datasets are large and broad, which requires filtering of available data. This study uses eight specific MODIS EOS satellite datasets.

LST: MOD11A1 (Wan & Hulley, 2015a), MYD11A1 (Wan & Hulley, 2015b), MOD11A2 (Wan & Hulley, 2015c) and MYD11A2 (Wan & Hulley, 2015d).

SREF: MOD09GQ (Vermote, 2015a), MYD09GQ (Vermote, 2015b), MOD09G1 (Vermote, 2015c) and MYD09G1 (Vermote, 2015d).

2.2.1 Secondary data sourcing

MODIS satellite data was retrieved from www.lpdaac.usgs.gov where the tile H18V2 was retrieved to include the point 69.75° latitude and 27.01° longitude, for the time period 5 March 2016 to 13 March 2016.

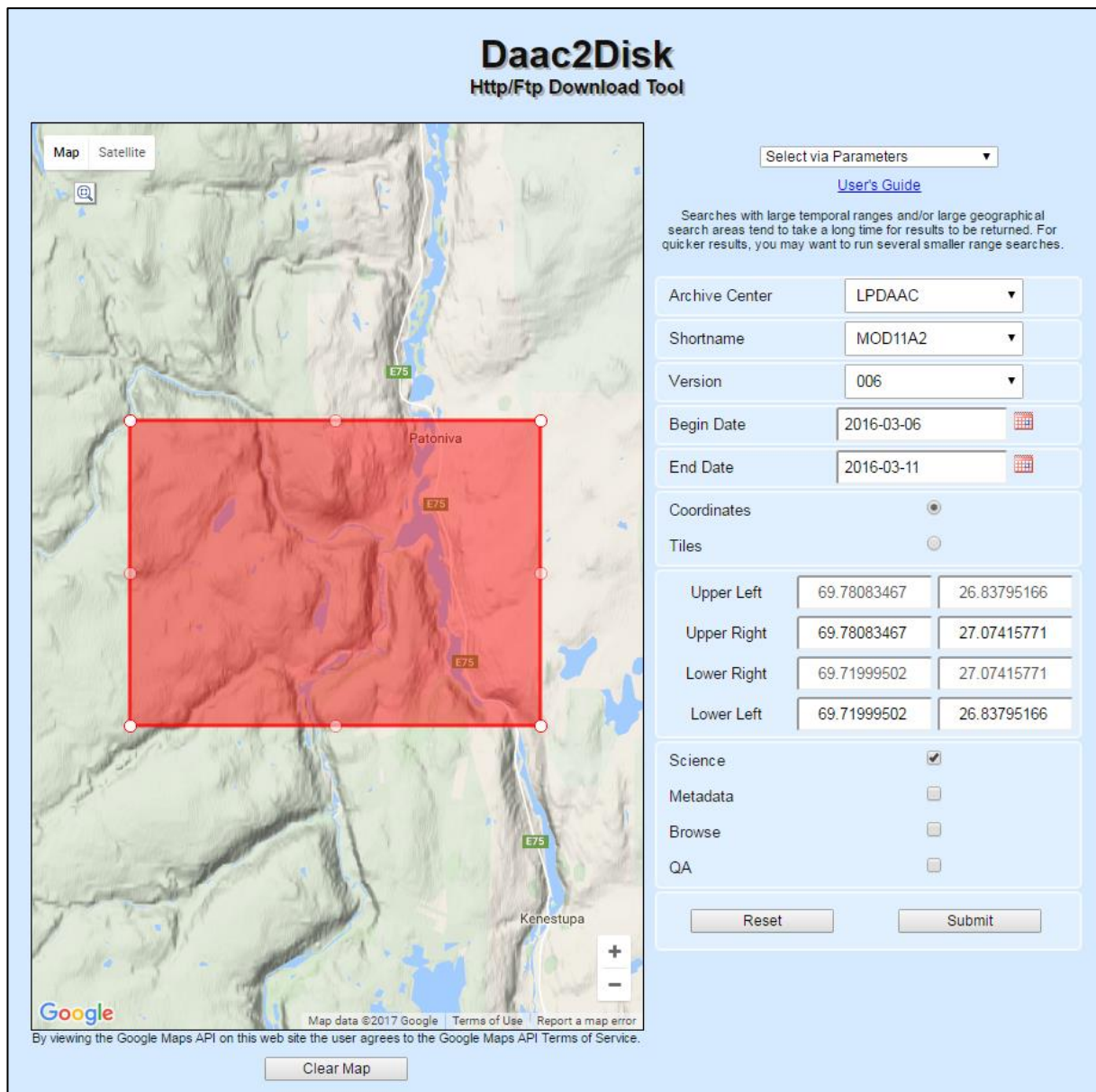


Figure 4: The order summary for MOD11A2. The same process was undertaken for all MODIS datasets: MOD11A1, MYD11A1, MOD11A2, MYD11A2, MOD09GQ, MYD09GQ, MOD09G1 and MYD09G1. Retrieved from 'DAAC2Disk | LP DAAC :: NASA Land Data Products and Services' (2014).

This download included various HDF4 images for differing data types within the eight datasets. All eight sets required unpacking using 7-Zip.

2.2.2 Secondary data elements

Table 3 shows all used subsets of the eight MODIS datasets. See Appendix B for the full dataset subsets.

SDS Layer Name	Description	Units	Data Type	Fill Value	Valid Range	Scaling Factor
MOD/MYD09GQ sur_refl_b01_1	Surface reflectance band 1	Reflectance	16-bit signed integer	-28672	-100 to 16000	0.0001
MOD/MYD09GQ sur_refl_b02_1	Surface reflectance band 2	Reflectance	16-bit signed integer	-28672	-100 to 16000	0.0001
MOD/MYD09Q1 Sur_refl_b01	Surface reflectance band 1	Reflectance	16-bit signed integer	-28672	-100 to 16000	0.0001
MOD/MYD09Q1 Sur_refl_b02	Surface reflectance band 2	Reflectance	16-bit signed integer	-28672	-100 to 16000	0.0001
MOD/MYD11A1 LST_Day_1km	Day Land Surface Temperature	Kelvin	16-bit unsigned integer	0	7500 to 65535	0.02
MOD/MYD11A2 LST_Day_1km	Day Land Surface Temperature	Kelvin	16-bit unsigned integer	0	7500 to 65535	0.02

Table 3: All MODIS subsets used for the eight separate datasets. Retrieved from lpdaac.usgs.gov (2014).

2.3 Data analysis

2.3.1 Heat map analysis

The interpolation method was Empirical Bayesian kriging, constantly used across all heat maps and isotherms. This method is considered the most accurate for smaller datasets, rather than inverse kriging and inverse distance weighting (Mirzael & Sakizadeh, 2015, p.2767).

2.3.2 Terrain analysis

Within ArcMap 10.4.1 Terrain analysis processes were preformed upon the digital elevation model (DEM). A DEM is often a raster image where continuous elevation values are given by z-values over a topographic surface (Wade & Sommer, 2006, p.52). The processes are used to evaluate topography in form and shape, resulting in terrain reclassification for many applications (DeMers, 2009, p.269). While elevation is the core of Terrain analysis, slope and aspect can be evaluated for a DEM using these tools. For analysis across Kevo valley topography, aspect and curvature are useful for further insight into ground influences upon LST and SREF.

2.3.2.1 Aspect

Aspect can be described as the orientation of a slope to a particular cardinal direction (DeMers, 2009, p.273). Sine of aspect gives a negative and positive value for a point where negativity is the westerliness of a point and positivity is the easterliness of a point. Cosine of aspect also gives positive and negative values for northerliness and southerliness respectively (Jenness, 2007, p.8). This transformation is described in Jenness' (2007) graph in Appendix C.

2.3.2.2 Curvature

Heywood et al (2011, p.207) describe curvature as the ‘rate of change of slope and aspect’.

Within ArcMap 10.4.1 curvature can be calculated as planform, profile or a combination of the two. This difference between these outputs is shown in Figure 5.

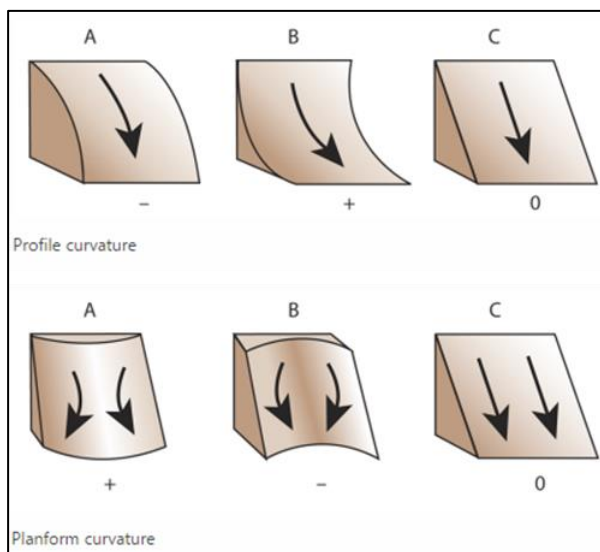


Figure 5: Two differing curvature outputs: planform and profile. Retrieved from ‘Curvature function’ (2016).

Positive curvature indicates the surface is convex at that cell. A negative curvature indicates the surface is concave at that cell. A value of zero indicates the surface is flat. (‘ArcGIS Desktop Help 9.3 - curvature’, 2011) This relationship is illustrated in Figure 6.

The negative and positive values are assigned to the severity of the topography. All topographic curvatures are exaggerated in Figure 5, and would be of the highest or lowest curvature values.

The combination output is known as general curvature and shown in Figure 6.

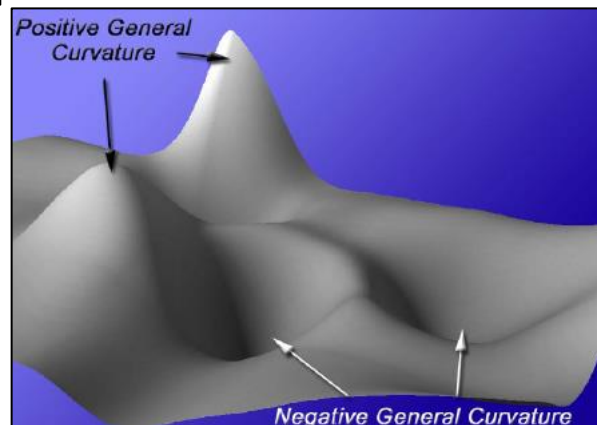


Figure 6: General curvature analysis output. Retrieved from Jenness (2007, p.13)

2.4 Radiation analysis

Irradiance inwards at the surface and irradiance reflected from the surface is measured in W/m². This measurement has been converted from arbitrary units using the equation below:

$$\frac{d}{10.8} \times \frac{1000}{n}$$

Where **d** = radiation difference and **n** = time period.

The time period (**n**) for the study is 30 seconds for irradiance and reflectance. The difference (**d**) is calculated from the difference between the two values recorded in the two 30-second time periods.

With the radiation composed of inward irradiance and outward reflectance, albedo for the area can be calculated from the following simple equation:

$$\alpha = \frac{F^+}{F^-}$$

Where α = **albedo**, F^+ = **radiation reflected** and F^- = **irradiance received**.

(Coakley, 2002, p.1915)

Albedo has been calculated from the irradiance dataset with the removal of the errors mentioned in Section 3.4. It can be used to compare to surface reflectance values from MOD09A1 and MOD09GQ.

2.5 Satellite data analysis

Data retrieval from the satellite HDF4 involved the data management section of the toolbox. Once downloaded, the HDF4 files were opened within ArcMap 10.4.1 and overlaid with 65 study points. The extraction tool from the spatial analyst toolbox assigns satellite values to each point residing in a specific satellite pixel. This resultant point layer is later converted within ArcMap into an Excel spreadsheet.

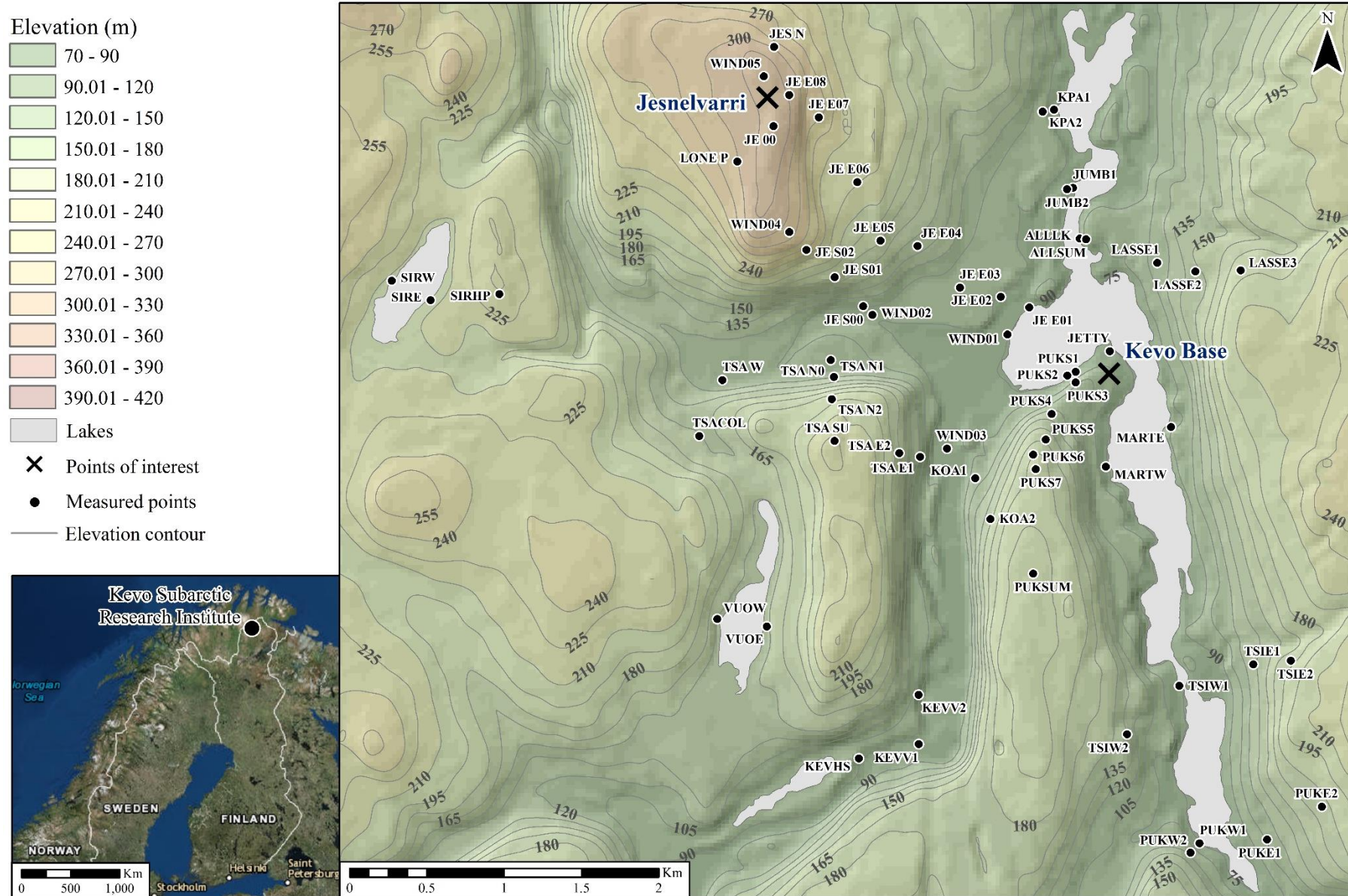
2.5.1 Cloud cover calculation

Conversion of sunshine minutes across my time period was necessary and the Swedish Meteorological and Hydrological Institute supplied it (STRÅNG, 2011). Data was given in the form of sunshine minutes in hour intervals. Cloud cover was given in oktas; thus, the sunshine minutes had to be divided into okta boundaries and an IF statement was implemented. If sunshine minutes in an hour were less than 7.5 minutes, then the okta value was 8. This rose in intervals of 7.5 minutes in an hour until 60 minutes where the okta value was at its lowest, 1. A tally for discrete variables was performed in Minitab to give a percentage of cloud cover for the week.

Chapter 3:

Results

Elevation for each measured point across Kevo Valley



Map 2: Elevation for each measured point across the study area. The map shows both elevation and point name for locational reference.

3.0 Results

3.1 Elevation

Map 2 represents the elevation of Kevo Valley. Its elevation derives from a DEM. When compared with global positioning system (GPS)-recorded elevation, it gives a R^2 value of 94.3% showing a close relationship with a few outliers; however, the GPS has a known error of 10 m (see Appendix D). The range of relief is from 70 m to 420 m; thus, the area can be described as hilly but not mountainous. This is represented by the colour scale and contours. All 65 points are labelled above. The points of highest and lowest elevation are JE 00 at 330 m and PUKS1 at 74 m.

3.2 Snow depth

Map 3 represents the average of snow depth recordings across each site. The average for snow depth was formed from the cardinal directions and depth at point. The lowest and highest snow depths observed were 11.66 m at JE 00 and 78.85 m at JES N. JES N is an isolated point of high depth on Jesnelvarri, which is why the heat map shows the smallest area of magenta. The majority of points here are better represented by JE 00, because Jesnelvarri is a high point across Kevo Valley and the snow is often removed by Aeolian forcing. JES N is in the wind shelter of Jesnelvarri, creating an anomaly of higher snow.

Generally, the heat map shows a north–south split in snow depths with higher depths in the south than that of the north. Such southerly points include PUKE2 at 66.89 m and VUOW at 68.72 m. The average snow depth across Kevo Valley is 54.06 m; however, the snow depth is controlled by various topographic and climatic factors, so averages are often spatially unrepresentative.

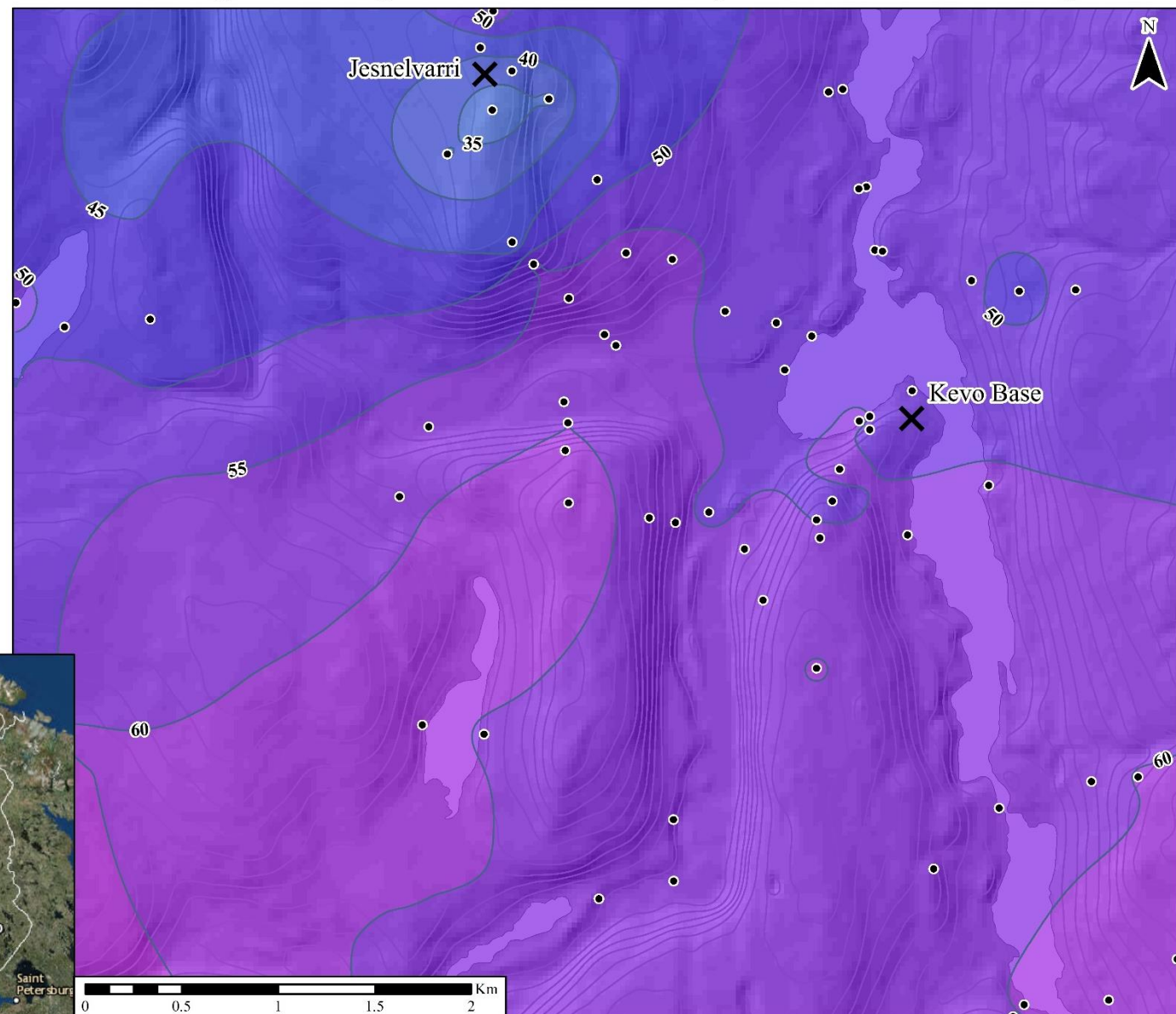
Snowpack depth (cm)

10.00 - 15.00
15.01 - 20.00
20.01 - 25.00
25.01 - 30.00
30.01 - 35.00
35.01 - 40.00
40.01 - 45.00
45.01 - 50.00
50.01 - 55.00
55.01 - 60.00
60.01 - 65.00
65.01 - 70.00
70.01 - 75.00
75.01 - 80.00
Lakes

- ✗ Points of interest
- Measured points
- Elevation contour
- Depth contour

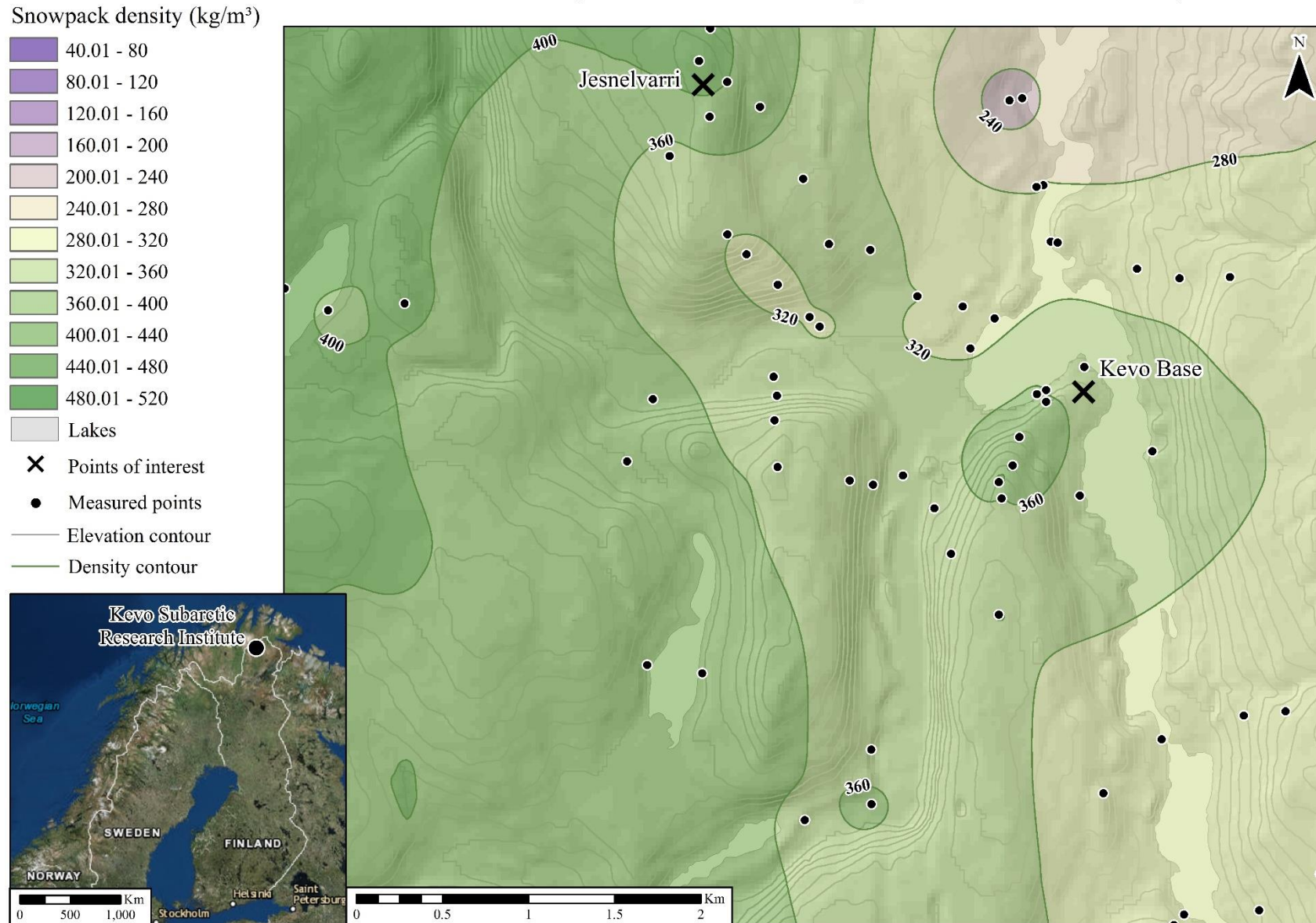


Average snow depth for each measured point across Kevo Valley



Map 3: Heat map of snow depth for each measured point.

Snow density for each measured point across Kevo Valley



Map 4: Heat map of snow density for each measured point.

3.3 Snow density

Map 4 represents snow density across the Kevo Valley. The maximum and minimum values are 488 kg/m³ at PUKS6 and 76 kg/m³ at KPA2. This minimum is shown in the top right corner of Map 4 with the purple trend. The majority of points (40 of 65) are above 320 kg/m³ or within the green bands; whereas 24 points of 65 are between 220 and 320 kg/m³ and only 1 point (KPA2) is below 220 kg/m³.

3.4 Surface radiation

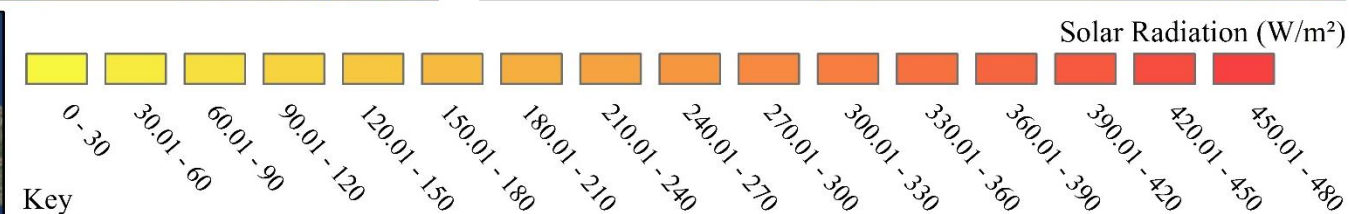
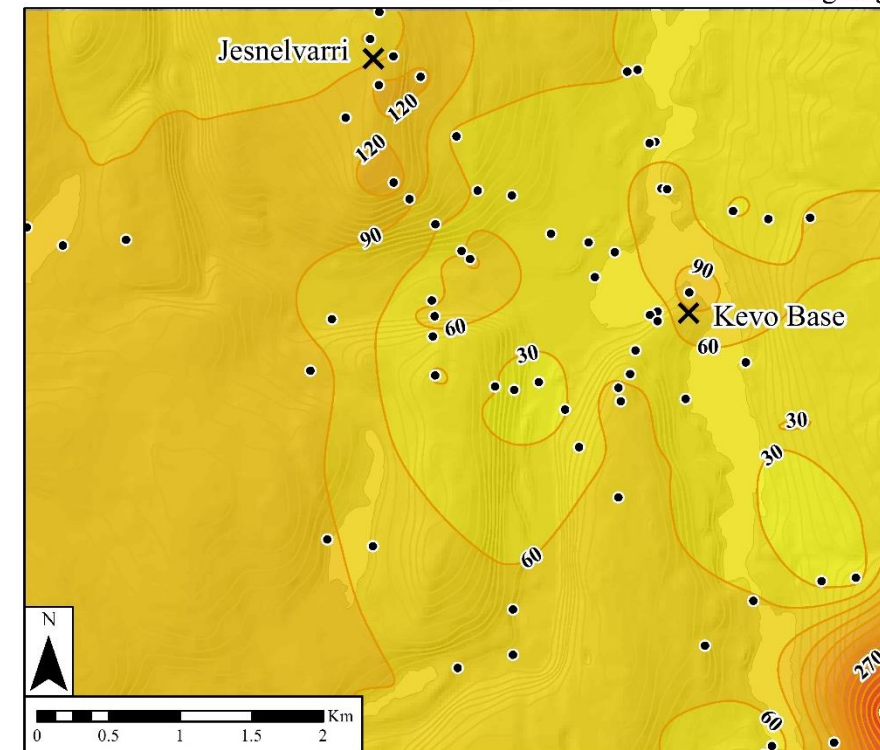
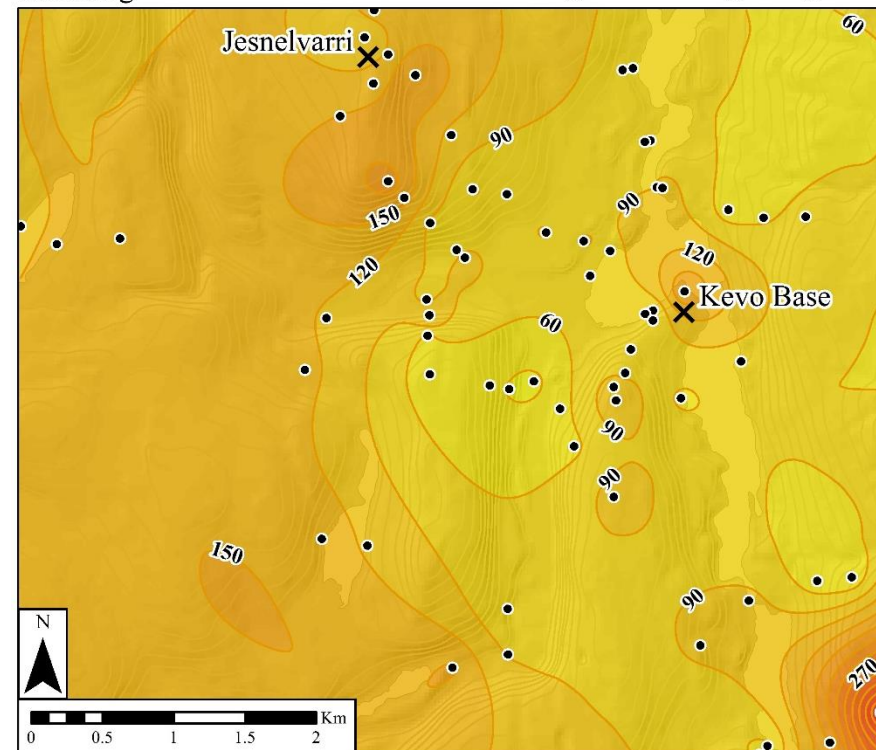
Map 5 shows surface radiation and surface reflectance. Maximums and minimums within the recorded data set for irradiance received (inwards) are 456.79 W/m² at PUKE2 and 18.52 W/m² at WIND03. Radiation reflected (outwards) is 472.22 W/m² at PUKE2 and 12.35 W/m² at WIND03. WIND03 shows the relationship of less reflection than absorption of radiation, while PUKE2 does not meet this and can be considered an anomaly within the dataset.

There are two similar points within the dataset: JE E05 and KEVV2. JE E05 recorded a received value of 55.56 W/m² while its reflected value was higher at 58.64 W/m². KEVV2 recorded a received value of 55.56 W/m² while its reflected value was higher at 61.73 W/m². Again, these values have been treated as anomalies within the dataset. Radiation received across the study week averaged 95.03 W/m² and for radiation reflected it averaged 65.82 W/m², both values are calculated after removal of anomalies. If PUKE2 is ignored, the western side of the map shows higher values than that of the east. This may be due to aspect of the ground and path of the sun.

Incoming

Incoming and outgoing solar radiation across Kevo Valley

Outgoing



Key

Lakes

× Points of interest

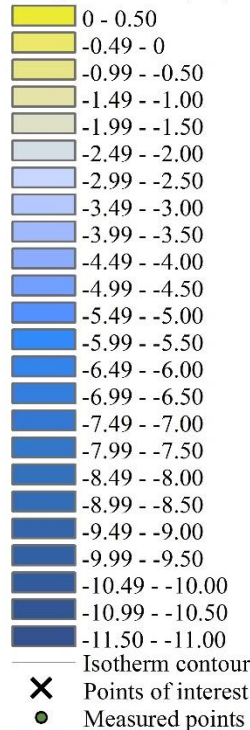
● Measured points

— Elevation contour

— Radiation contour

Map 5: Heat map of solar radiation both incoming and outgoing, for the study area.

Top of the snow pack
temperatures (°C)



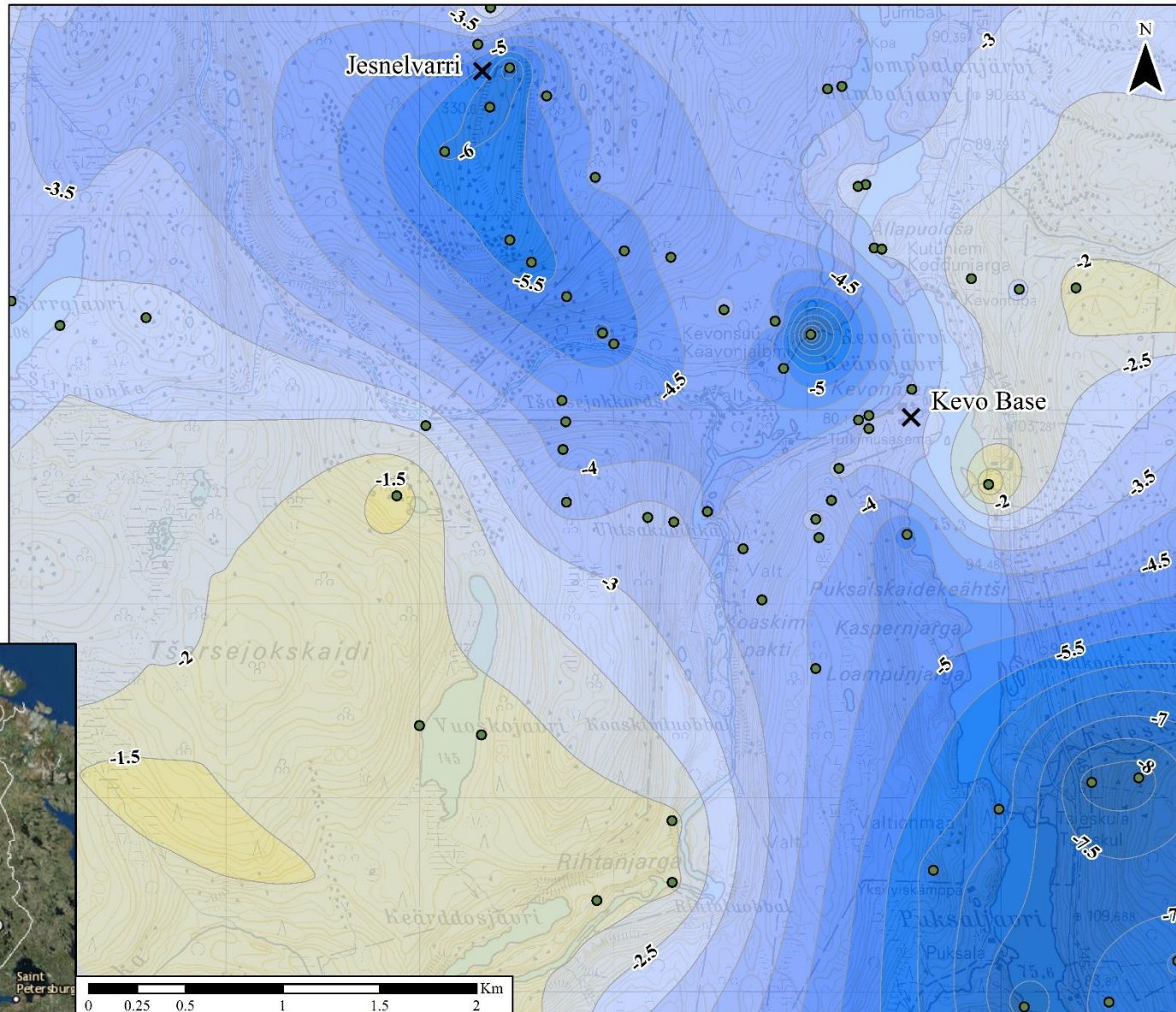
Isotherm contour

X Points of interest

• Measured points



Isotherm map for top of snowpack temperature in °C



Map 6: Isotherm map for temperature at the top of the snowpack.

3.5 Snowpack surface temperature

Map 6 represents an isotherm map for temperatures at the surface of the snowpack. The two extremes of the coldest and the warmest sites are JE E01 at -11.50 °C and MARTE at 0.50 °C. However, the difference between MARTE surface temperature and bottom temperature is -0.70 °C, where the base temperature is cooler. For this reason, it can be considered an anomaly, because the next highest temperature is -0.25 °C at TSACOL.

On average, snowpack surface temperature is -3.96° C, and an ordinal split can be seen where areas in the north east and south west are warmer than those in the north west and south east. However, the density of points is not evenly spread and the isotherm is at its most accurate for areas around Kevo base and north-westerly towards Jesnelvarri. Points at higher elevations clearly show colder temperatures.

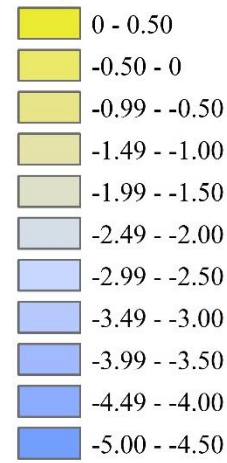
3.6 Snowpack base temperature

Map 7 can be compared to Map 6 because the colour range is equal for each colour and temperature class. The coldest and warmest sites are JE 00 at -5.00 °C and PUKE2 at 0.30 °C, respectively. The average snowpack base temperature is -0.69 °C. With regards to the distribution of the isotherm bands on Map 7, most areas are warm and within yellow bands other than those at Jesnelvarri peak and close to some bodies of water; namely, the river running north–south, between the KOA and TSA E transects.

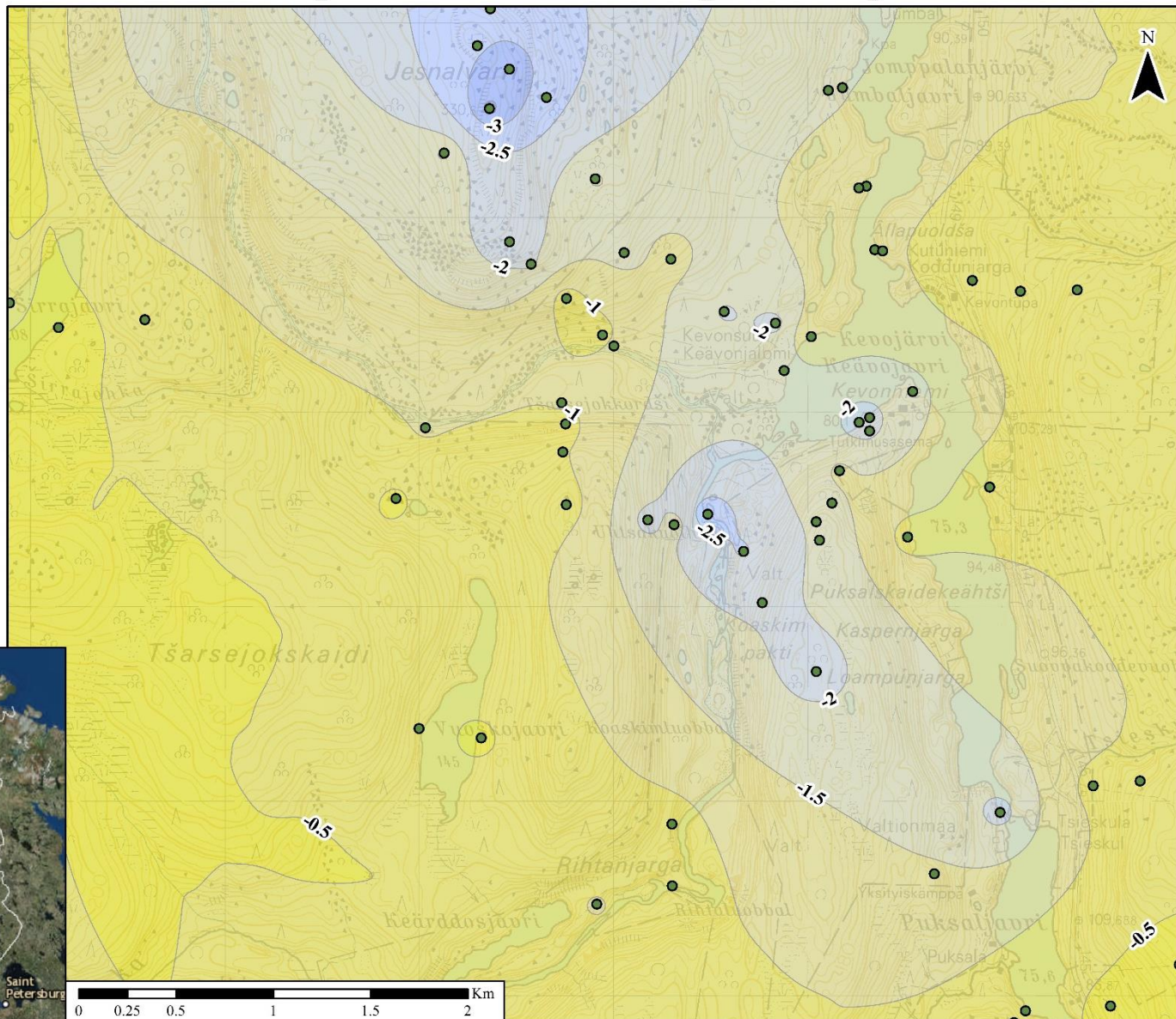
Snowpack surface and base temperatures will be used for further analysis of snow insulation and LST MODIS comparison. Temperature anomalies at JES N and MARTE will be removed; specifically, where JES N base temperature was -2.90 °C and surface temperature was warmer at -1.00 °C.

Isotherm map for bottom of snowpack temperature in °C

Bottom of the snow pack
temperatures (°C)

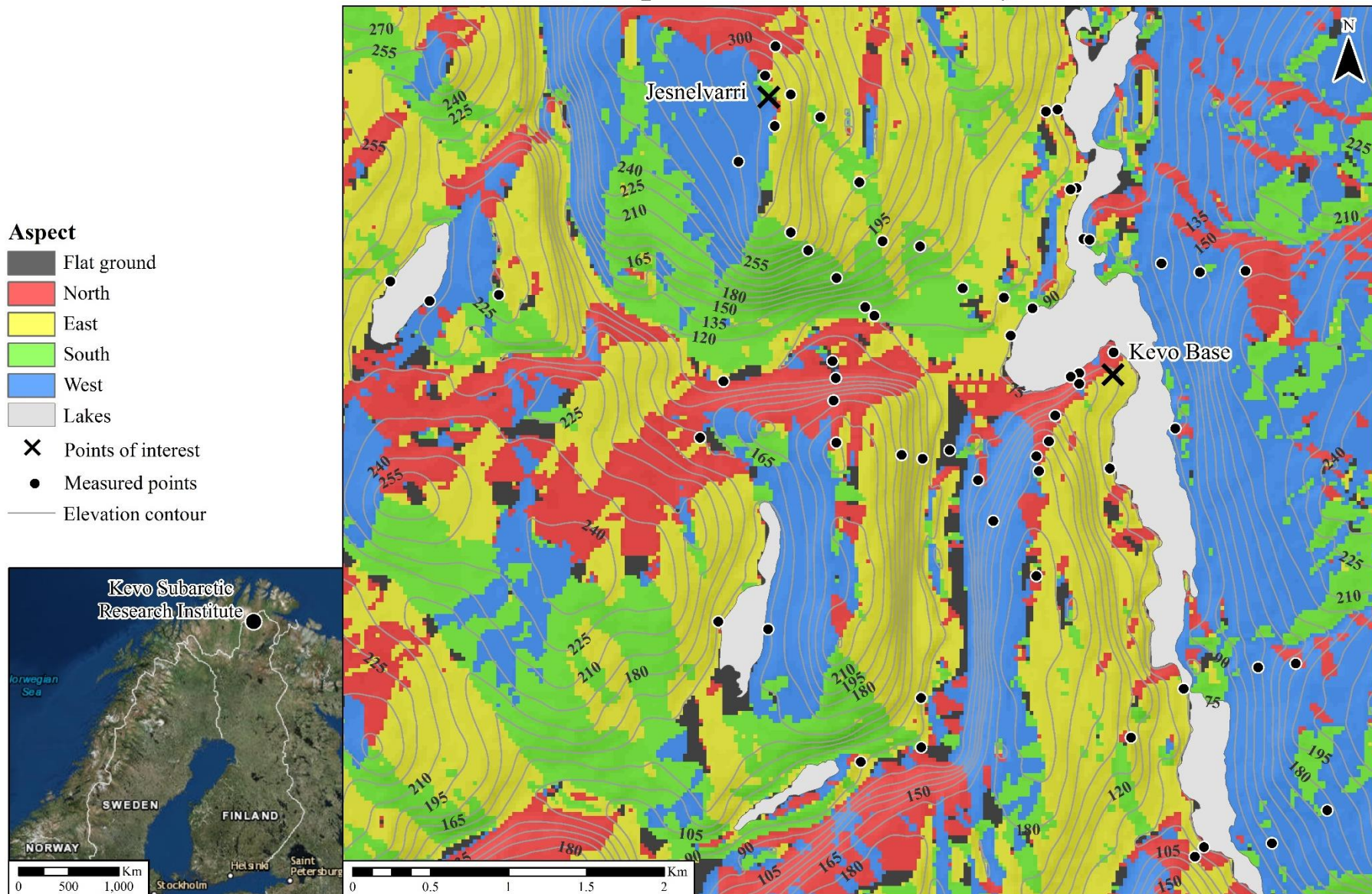


- Isotherm contour
- ✗ Points of interest
- Measured points



Map 7: Isotherm map for temperature at the bottom of the snowpack.

Aspect of the Kevo Valley terrain



3.7 Aspect

Map 8 represents the aspect for Kevo Valley. The map is complete with contour lines and hill shading to give an effect of relief alongside the aspect values. This map was used to export cardinal data for each separate measured point, which is further processed into sine and cosine values for aspect.

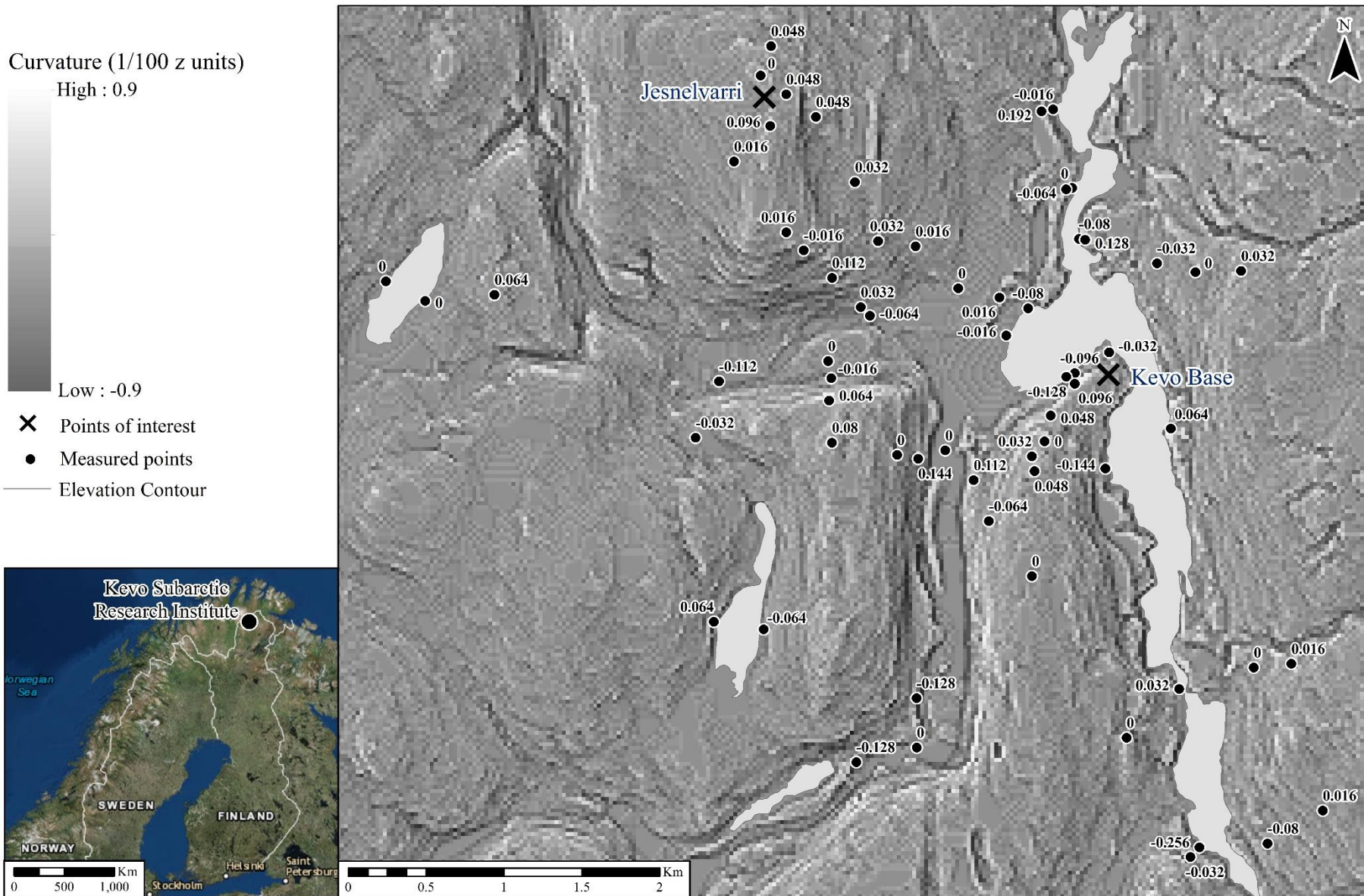
3.8 Curvature

The curvature values of each measured point are shown in Map 9, where a maximum point of convex curvature is 0.192 1/100 z units at KPA2 and a minimum point of concave curvature is -0.256 1/100 z units at PUKW1. The average curvature across all 65 points is -0.317 1/100 z units.

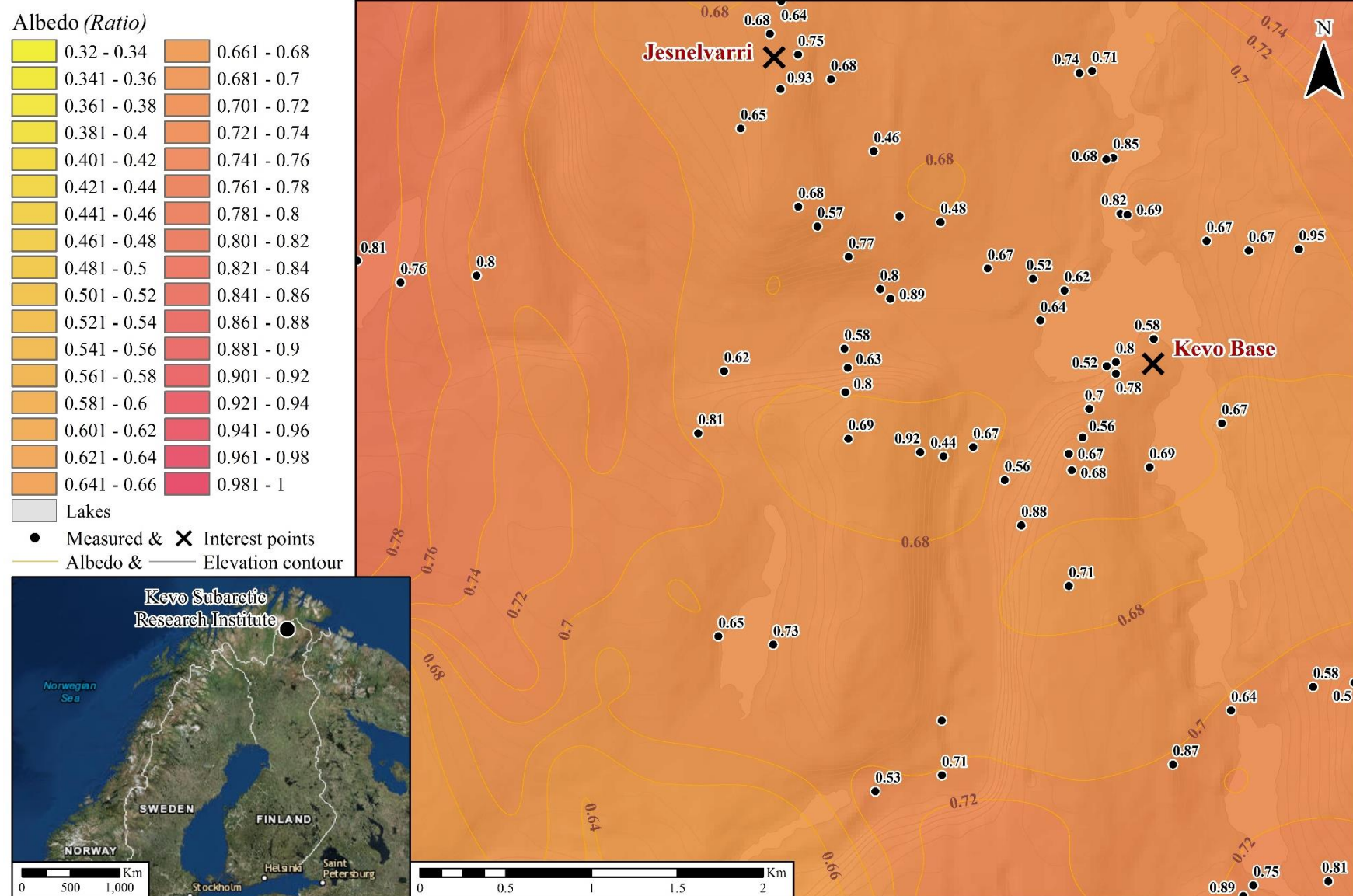
3.9 Albedo

Map 10 shows a heat map for Albedo as calculated from an anomaly-free solar irradiance and reflectance dataset. The kriging scale is comparable across all satellite albedo and manual albedo maps varying from yellow to red. The maximum point data recorded is 0.95 at LASSE3 while the minimum point is 0.43 at TSA E1. The average manual albedo recorded is 0.70. Albedo does tend to be spatially higher on east face slopes when compared with the aspect Map 9. This could be due to sunlight hours in the day and the point at which the sun rises and sets.

Curvature of each measured site across Kevo Valley terrain



Manual albedo for surface across the Kevo Valley



Map 10: Manual Albedo heat map for study area.

Chapter 4:

Analysis

4.0 Satellite analysis and interpretation

To address the overall aim, it is fundamental to undertake satellite sensor analysis. The MODIS datasets are within the MOD11/MYD11 and MOD09/MYD09 packages for daily and composite representation.

4.1 Satellite spatial and temporal coverage

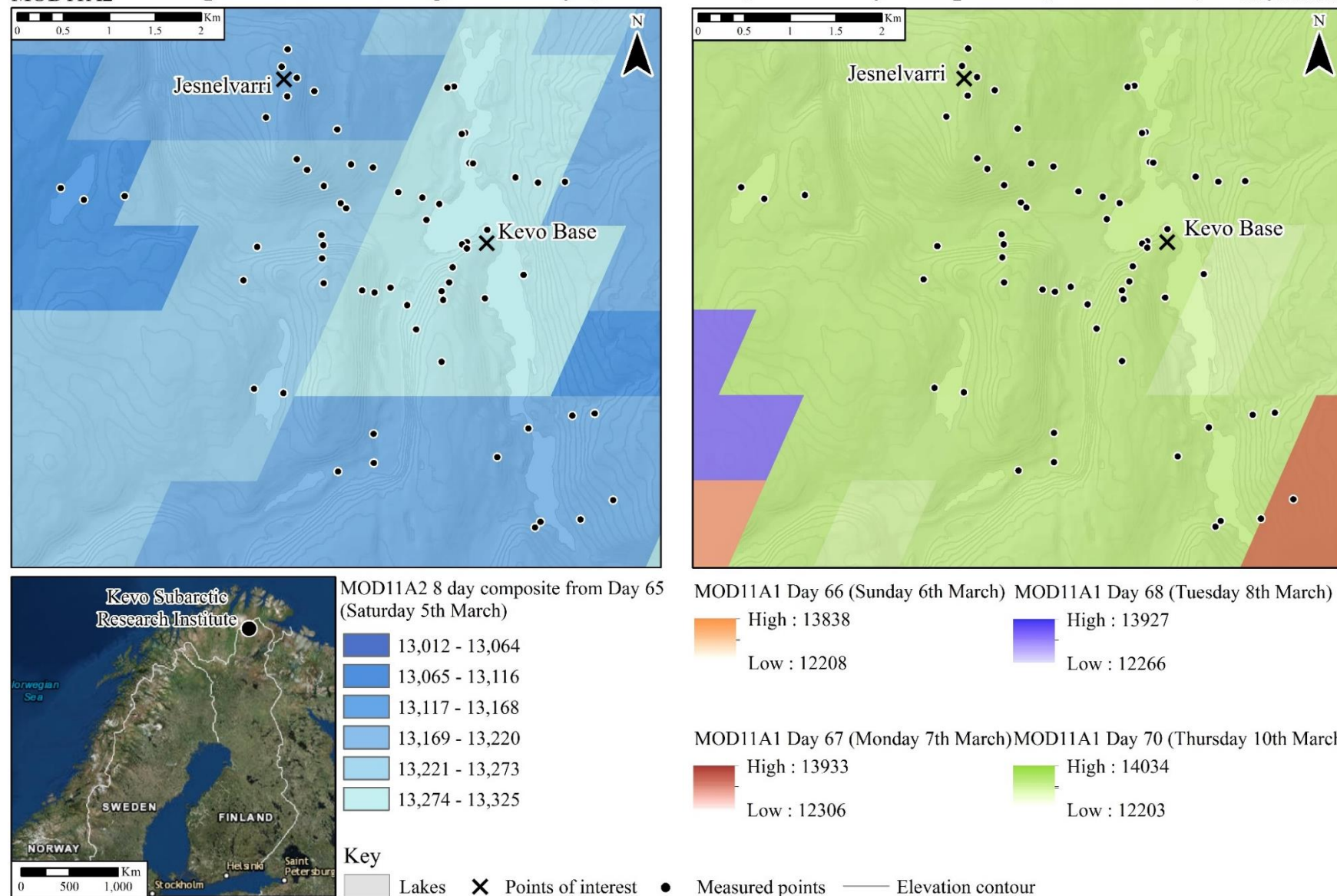
Weather often affects satellite visibility, with cloud cover causing much of the blocking. Table 4 is a tally table for cumulative cloud cover as measured in oktas. It shows that for 89.49% of the study week, Kevo Valley was at 8 oktas, which is full cloud cover.

<i>Cloud Cover (okta)</i>	<i>Count</i>	<i>Percentage (%)</i>	
1	2	1.17	
2	4	2.34	
4	2	1.17	
6	2	1.17	
7	8	4.68	
8	153	89.47	The average time difference between Terra and Aqua satellites for Kevo Valley is 18 minutes based on the passing time between MODIS Terra at 12:12pm and MODIS Aqua at 12:30pm. This was calculated from the satellite HDF4 'Day_view_time' layer, and is based on day 70 (Thursday, 10 March 2016) clear sky LST observation (see Appendix E).

Table 4: Cloud cover percentage for okta value throughout the study week.

Map 11 shows the difference between daily and composite data availability. Composite can give values across the whole study area for the week, whereas the only daily layer with good coverage is day 70, due to cloud contamination, similar to Hachem et al (2012, p.58). For this reason, the only dataset available for overall valley analysis is MOD11A2; however, there is opportunity for a micro study upon the day 70 manual transect and MOD11A1.

MOD11A2 Comparison of coverage for daily (MOD11A1) and 8 day composite (MOD11A2) MOD11A1



Map 11: Comparison of MOD11 coverage for both daily and composite sensor data.

4.2 Terra, Aqua and field data comparisons

Table 5 provides a correlation matrix for all variables that are thought to influence each other.

	Temp Bottom	Temp Top	MOD11A2	MYD11A2	Density	Albedo	MOD09Q1	MOD09GQ	MYD09Q1	MYD09GQ	Depth	Elevation	Curvature	Sine Aspect	Cosine Aspect	DistLake
Temp Bottom	—															
Temp Top	0.091	—														
MOD11A2	-0.114	0.231	—													
MYD11A2	-0.269	0.308	0.697	—												
Density	-0.103	0.158	-0.271	-0.100	—											
Albedo	0.012	0.025	-0.155	-0.181	-0.050	—										
MOD09Q1	-0.145	-0.080	-0.317	-0.086	0.208	0.005	—									
MOD09GQ	-0.017	0.101	0.106	0.061	0.082	0.210	-0.039	—								
MYD09Q1	-0.141	-0.277	-0.405	-0.220	0.140	-0.020	0.609	0.099	—							
MYD09GQ	0.068	0.184	0.070	0.092	0.279	0.090	0.246	0.452	0.124	—						
Depth	0.375	0.119	0.127	-0.189	-0.113	-0.113	-0.237	-0.110	-0.274	-0.129	—					
Elevation	-0.281	-0.138	-0.549	-0.178	0.375	0.089	0.492	-0.081	0.437	0.185	-0.381	—				
Curvature	-0.178	0.102	-0.001	0.090	-0.108	-0.034	0.113	-0.096	0.109	-0.172	-0.156	0.342	—			
Sine Aspect	-0.014	-0.104	-0.022	0.165	0.161	-0.267	-0.042	0.004	0.084	-0.072	-0.030	0.022	-0.067	—		
Cosine Aspect	0.010	-0.064	0.152	0.156	-0.218	-0.040	-0.061	-0.056	-0.056	0.069	0.146	-0.007	-0.073	0.137	—	
DistLake	-0.306	-0.164	-0.401	-0.011	0.231	-0.035	0.380	-0.233	0.234	0.046	-0.264	0.751	0.235	0.026	0.030	—

Table 5: Correlation Matrix for all variables.

The Table 5 matrix provides R-values to indicate the relationship between two variables. Where R-values are between 0.40 and 0.59, they can be considered as having moderate correlation, while 0.6 to 1.00 can be considered as a having strong to very strong correlation (Evans, 1996). Interest in the data for comparison between Terra and Aqua has been highlighted in green, while comparisons between daily and 8-day composite variables are highlighted in red. A strong correlation would be expected for these two variable types because the 8-day test is a composite of the daily, and Terra and Aqua have only an 18-minute gap between pass over times for Kevo Valley. However, while Terra and Aqua show a moderate to strong correlation, daily and composite data are not correlated as expected, which brings into question the composite methods and the reliability of these data sets. The correlation matrix also shows moderate to strong relationships between variables in bold, these variables do not relate to the satellite type and version comparison. These variables are best considered alongside other the rest of the data using Principal Components Analysis.

Considering the interesting correlation coefficients in Table 5, further analysis was conducted on the differing satellites and their daily and composite products. Tables 5 and 6 have a *t* test *p*-value matrix that shows whether there is a significant statistical difference between each variable. If the value in the cell is a *p*-value higher than 0.05, then the two are not significantly statistically different (Ofwungu, 2014, p.54).

4.2.1 Surface reflectance

	<i>Manual</i>	<i>MOD09GQ</i>	<i>MYD09GQ</i>	<i>MOD09Q1</i>	<i>MYD09Q1</i>
<i>Manual</i>		0.001	0.000	0.003	0.000
<i>MOD09GQ</i>	0.001		0.054	0.604	
<i>MYD09GQ</i>	0.000	0.054			0.037
<i>MOD09Q1</i>	0.003	0.604			0.543
<i>MYD09Q1</i>	0.000		0.037	0.543	

Table 6: *P* value table showing the significance of statistical difference between SREF satellites and products.

When compared to all satellite products, Table 6's manual data shows a statistically significant difference, which seems contradictory when considering the *p*-values between the satellite types and products. MODIS Terra and Aqua for daily and composite data is considered not statistically different: daily data from Terra and Aqua gives a *p*-value of 0.054, while composite data from Terra and Aqua gives a *p*-value of 0.543. These values have been highlighted in orange. This relationship between Terra and Aqua is expected to produce similar data, as the time gap between collections for Kevo Valley is only 18 minutes, as calculated in Section 4.4.1. Furthermore, this data collected on Terra and Aqua is expected to show synergy for enabling cloud free data for MODIS sensors in general (National Snow and Ice Data Center, n.d.).

Next, considering the statistical significance between daily and composite data for Terra and Aqua satellites, the results are variable. Terra satellite shows a p -value of 0.604 for the difference between daily and composite data, which is a value of no statistically significant difference. However, when considering Aqua satellite, the p -value for daily and composite data is 0.037, which does show statistical significance. Statistical significance here could be expected due to the 8-day composites of daily data, where daily synoptic conditions may control albedo and a composite may remove this variation, as its aim is to show the best of the cloud-free days. However, as a composite it may be expected that it should give good coverage for a week regardless of synoptic fluctuation. It is arguable that with p -values such as those shown in yellow whether either data package could be appropriate for spatial analysis.

4.2.2 Land surface temperature

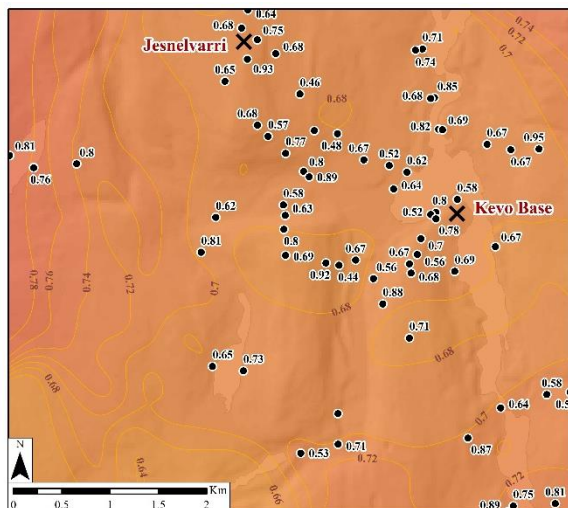
	<i>Manual</i>	<i>MOD11A2</i>	<i>MYD11A2</i>
<i>Manual</i>		0.000	0.000
<i>MOD11A2</i>	0.000		0.000
<i>MYD11A2</i>	0.000	0.000	

Table 7: *P* value table showing the significance of statistical difference between LST satellites.

Table 7 shows the t test matrix for manual LST and Terra and Aqua satellite datasets for the 8-day composite. For all variables in the table, there is statistical significance with a p -value of 0.000 for all t tests. This difference between manual data initially indicates there is variance between ground manual data recorded and that of the satellite composite.

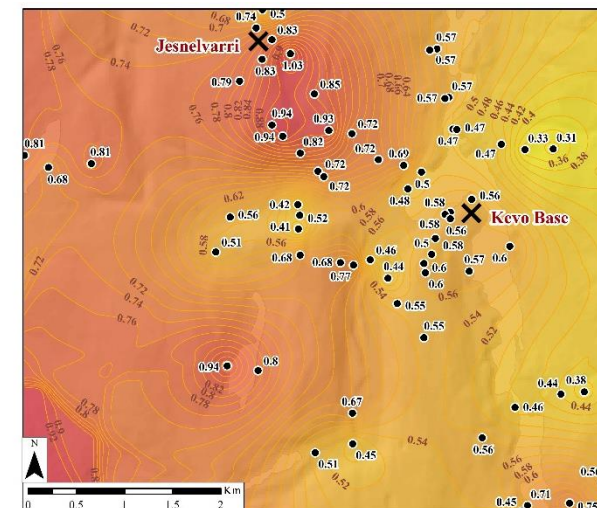
However, as with SREF, the difference between Aqua and Terra would be expected to be of no significance: 18-minute capture times. This is not the case for LST. For continuity, Terra data only will be used for analysis of LST and SREF. The average of MODIS Terra and Aqua has been done in studies such as Hachem et al (2012, p.57). In Hachem et al's (2012) study, Terra and Aqua values for similar satellite MODIS products were highly correlated from the beginning, as seen in Table 4. This is not the case for Kevo valley. Terra satellite usage is most appropriate because it is a land-based satellite, and also records morning products (Reese, 2016). It is suited to 69% of points recorded for Kevo Valley.

4.3 Albedo vs MOD09



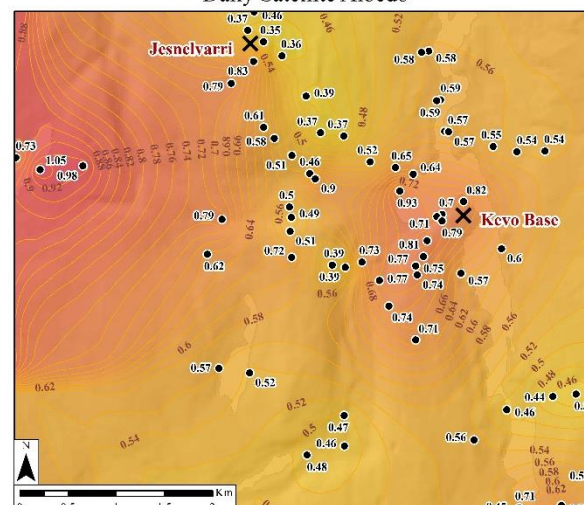
Manual Albedo

Albedo comparison for each measured point across Kevo Valley



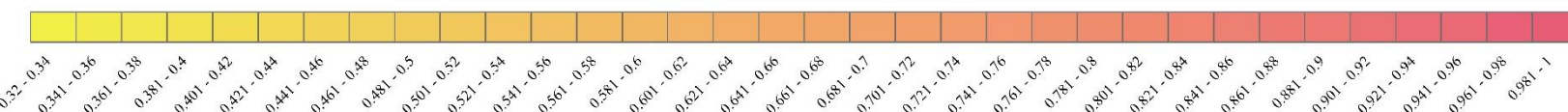
8 Day Composite Satellite Albedo

Daily Satellite Albedo



Albedo (Ratio)

- Lakes
- X** Points of interest
- Measured points
- Albedo contour



Map 12: Visualisation of MODIS Terra albedo comparison to manual albedo data.

4.3.1 Albedo analysis and further interpretation

Map 12 is the composition of manual, daily satellite and composite satellite shortwave albedo recordings, where bands measured are 1 (620–670 nm) to 2 (841–876 nm) for the satellite datasets (Vermote, 2015) and 400–1050 nm wavelength for the manual dataset (Delta T, 2000) as given by a current manual for the current version (ES2) of the older model used. Manual albedo has a range from 0.44–0.95; while this is wide, it is the most compact out of all area albedo datasets. With daily satellite albedo (DSA) and composite satellite albedo (CSA) have a range of 0.35–1.05 and 0.31–1.03, respectively.

Firstly, it is important to recognise the two impossible values within both satellite datasets. Albedo for a surface cannot be above 1.00 at the wavelengths measured, but these points were JE E07 at 1.03 and SIRE at 1.05. While these two values may be satellite anomalies, it does raise questions about the accuracy of this dataset. While they do fall within Lillesand's calibration error of 5%, SIRE is at the top end, suggesting perfect reflectance of 1.00 if 5% were to be removed due to error, which is an impossible value. These two points will be removed from principal component analysis (PCA).

The relationship between manual and satellite datasets can be quantified using correlation coefficients from Table 8.

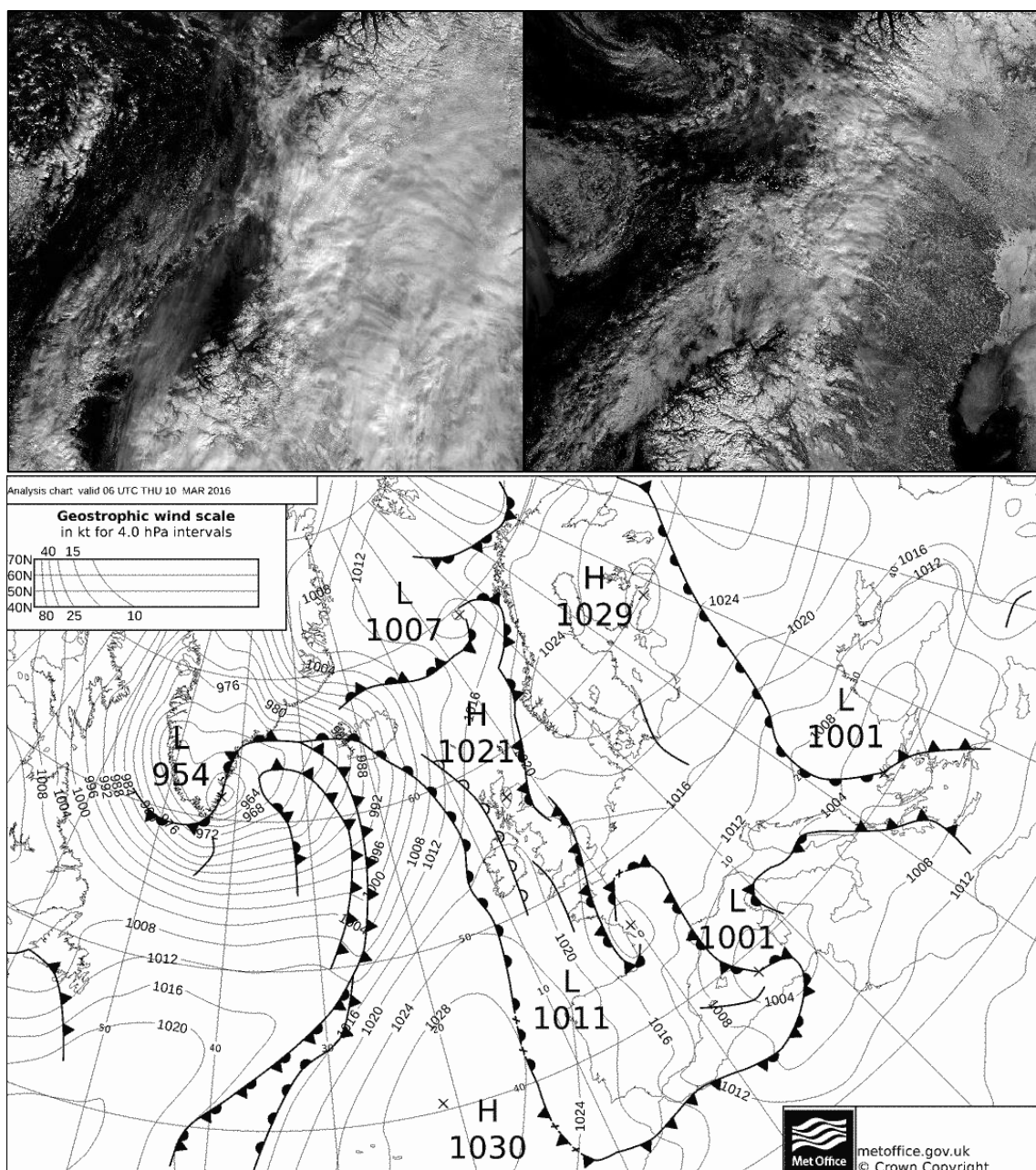
	<i>Manual</i>	<i>MOD09GQ</i>	<i>MOD09Q1</i>
<i>Manual</i>	—————	0.210	0.005

Table 8: Albedo correlation coefficients for manual vs satellite datasets.

The following points can further explain these weak values.

The satellite datasets shows far larger albedo variation compared to manual albedo, with a heat map kriging showing this. Shades of deep red and yellow can be seen for the two satellite datasets in contrast to the manual dataset. The average albedo for DSA and CSA is 0.61 and 0.62, respectively; whereas the recognised albedo for snow is from 0.80–0.90 (Wiscombe & Warren, 1980). The manual data average is 0.20 below this value, approximately 14% closer than either of the satellite datasets. One reason for this could have been cloud contamination upon satellites at 89.47% cover for the week, taken from Table 3.

While all pixels are recorded within the satellite dataset, the large-scale view of tile H18V2 shows cloud cover for day 66 in contrast to day 70 (see Figure 7). Evidence of cloud cover is supported within the LST satellite recordings where only day 70 recorded pixel values across the whole region which coincides with a high-pressure system within the synoptic charts. Similar analysis by Serreze and Barry (2014, p.29) further cements these views. This indiscrimination between snow surfaces and clouds is clear for satellite retrieval at high latitudes, where records of visible wavelengths for both features, show the same reflectance. (Serreze & Barry, 2014, p.57).



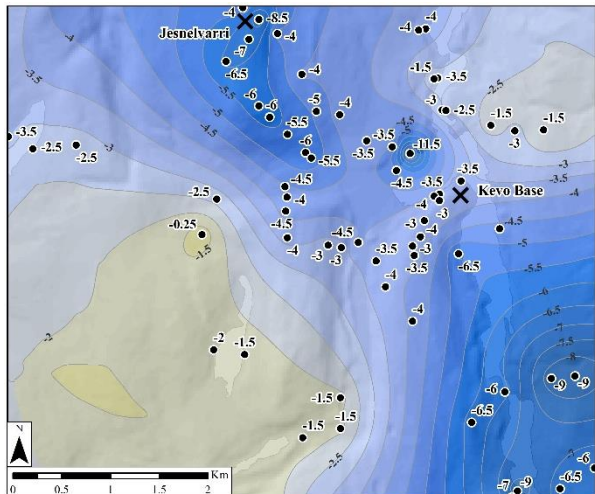
Lastly, a weak elevation forcing upon albedo can be shown within the daily satellite high to the south of Kevo Base. This is the PUKS transect from PUKS1 to PUKSUM. Table 9 shows the related values. Inconsistency across datasets means this trend is not as clear as first thought. While topographic features from Maps 2 and 8 have been compared to Map 12, curvature shows no trend within this single variable but may be relevant as part PCA.

<i>Point</i>	<i>Elevation (m)</i>	<i>Manual</i>	<i>DSA</i>	<i>CSA</i>
<i>PUKS1</i>	74	0.8	0.70	0.58
<i>PUKS2</i>	83	0.52	0.71	0.58
<i>PUKS3</i>	92	0.78	0.79	0.57
<i>PUKS4</i>	120	0.7	0.81	0.58
<i>PUKS5</i>	171	0.56	0.75	0.50
<i>PUKS6</i>	184	0.67	0.77	0.60
<i>PUKS7</i>	189	0.68	0.74	0.60
<i>PUKSUM</i>	200	0.71	0.71	0.55
<i>Average</i>	—	0.68	0.75	0.57

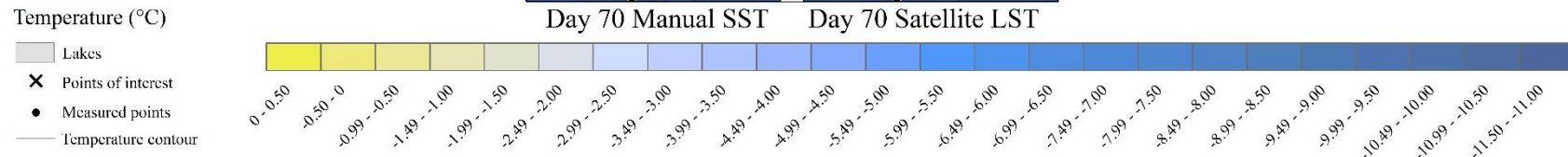
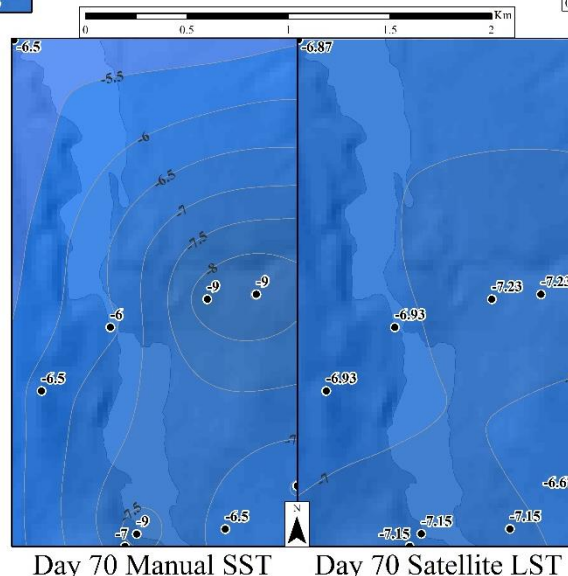
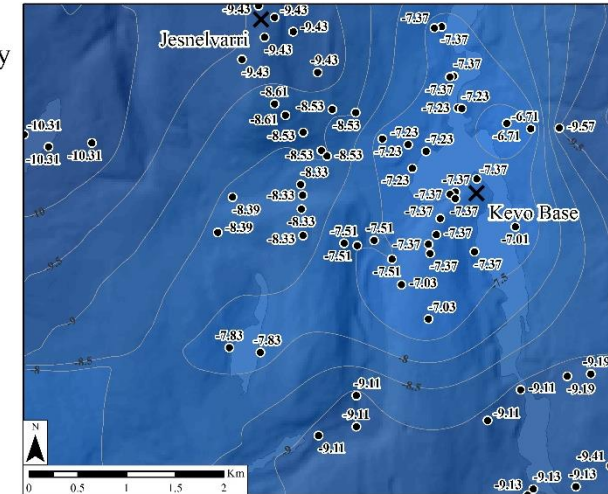
Table 9: PU KS transect albedo vs elevation analysis.

It may also be expected that DSA and CSA would be similar in readings as CSA is a composite of DSA. However, from further MOD11 interpretation, composite datasets comprise the best days, most of which are expected to be cloud free. While the difference between cloud free and cloudy is clear for LST (MOD11) data, this is not the case for MOD09 where all pixels recorded values. An explanation could be that snow albedo and cloud albedo are similar and the satellite datasets struggle to remove cloud values for Arctic datasets. Serreze and Barry (2014, p.57) further reinforce this dataset disparity

4.4 Surface temperature vs MOD11



Surface Temperature comparison
of each measured point across Kevo Valley
Including day 70 micro study



Map 13: Visualisation of MODIS Terra LST comparison to manual SST data. Daily data is used within a day 70 micro study.

4.4.1 LST analysis and further interpretation

Map 13 is the composition of manual, daily satellite and composite satellite surface temperatures where manual data is a recording of the snow surface temperature and satellite datasets are a recording of the LST. There is a direct comparison between manual surface temperature (MST) and composite satellite temperature (CST). However, due to cloud cover, full daily satellite temperature (DST) pixel coverage for MOD11 is only available for day 70 or Thursday, 10 March 2016. As a result, a micro comparison has been featured in the centre of the map.

The relationship between manual and satellite datasets can be quantified using correlation coefficients from Table 10.

<i>Manual</i>	<i>MOD11A2</i>	<i>MOD11A1 – Day 70 only</i>
<i>Manual</i>	0.231	0.580

Table 10: LST correlation coefficients for manual vs satellite datasets.

Manual snow surface temperature is the result of Map 6 with the removal of anomalous points. The general trend is similar with a range from -0.25°C to -11.5°C, while CST shows a wider range at -6.71°C to -10.31°C. To compare, temperatures between MST and CST are -4.30°C and -8.26°C, respectively. This is a difference of almost double MST, with CST recording lower temperatures where the average difference between each point is -4.10°C. A comparison here can be drawn between the recording difference for CST and the amount of cloud cover for the week in Table 3, where there is 89.47% cloud cover and the difference between the averages is 92% of the value of MST. For this similarity, it can be suggested that for composite coverage the cloud cover affected recordings or the composite is only made of clear days. The initial explanation seems unlikely because MOD11A1 (DST) is designed to remove cirrus influence (Wan, 2013).

However, upon coverage analysis in Map 11, the DST failed to record pixel values for the whole region, other than day 70, where temperature averages across the transect were -8.97°C (DST) and -7.28°C (MST), which is in keeping with the CST. It seems likely that weekly composites could be based upon one clear day in this week, overlooking cloud covers effect upon MST. This relationship is in keeping within Serreze and Barry's (2014, p.24) findings that the Arctic is a 'cloudy place' with the Atlantic sector having an estimated 80% cloud cover over a year, resulting in a thermal isolation of the arctic when shrouded in cloud.

This process is known as cloud radiative forcing, where clouds result in a warming effect at the surface. This process is due to the trapped long wave radiation between the surface and the cloud base, where long wave radiation is emitted from a high albedo surface, such as snow, and struggles to escape through cloud base, further reflecting back towards the surface (Serreze & Barry, 2014, p.139; Curry, 1996). This process is a positive feedback loop as explained in Figure 1. The process is further intensified by a high albedo of thick cloud cover, which is commonly 70% to 80% albedo (O'Hare & Sweeney, 1986). This increases the reflectance of the initially emitted waves from the ground, further blocking the passage through the cloud layer.

For the three-way surface temperature comparison in Map 13, clearly manual data can record such temperatures under cloud radiative forcing conditions whereas satellites cannot record daily pixel values for cloud covered days and can only composite from clear days. For example, day 70, a day with no obvious cloud radiative forcing and strong data correlation shown by Table 10. It can, therefore, be considered that radiative forcing can never be represented for satellite LST data from the MOD11 sensor.

4.5 Principal Components Analysis

This is a mathematical technique for data reductions, meaning the process will produce a smaller set of uncorrelated variables—known as principal components—where they are from the larger set of original variable where some are redundant or intercorrelated (Ofungwu, 2014, p.438) (see Table 5).

4.5.1 Principal Component Analysis for non-MODIS variables (PCA1)

Principal Component Analysis: Temp Bottom, Temp Top, Density, Albedo, Depth, Elevation DEM, Curvature, Sine Aspect, Cosine Aspect, Distance from Lake and Cloud Cover

Eigen analysis of the Correlation Matrix
60 cases used, 5 cases contain missing values

Eigenvalue	2.7101	1.5816	1.3700	1.2684
Proportion	0.246	0.144	0.125	0.115
Cumulative	0.246	0.390	0.515	0.630

Variable	PC1	PC2	PC3	PC4
Temp Bottom	-0.326	0.092	0.056	-0.177
Temp Top	-0.029	0.613	-0.148	-0.206
Density	0.212	0.038	0.242	-0.702
Albedo	0.012	-0.227	-0.611	-0.155
Depth	-0.427	0.201	0.034	0.004
Elevation DEM	0.515	-0.148	0.010	-0.057
Curvature	0.310	0.356	-0.161	0.347
Sine of Aspect	-0.021	-0.052	0.682	-0.006
Cosine of Aspect	-0.127	-0.116	0.183	0.511
Distance from Lake	0.467	-0.158	0.085	0.089
Cloud Cover	0.264	0.576	0.104	0.129

+ve CosX = Northerliness +ve SinX = Easterliness
-ve CosX = Southerliness -ve SinX = Westerliness

Figure 8: Principal Component Analysis for all non-MODIS variables. Full PCA in appendix F.1.

This PCA compares the 10 ground variables, not including satellite information for albedo and LST. PC1 forms 24.6% of the correlation forcing. This component consists of a relationship where an increase in elevation (0.515) increases the distance from valley lakes (0.467) represented by positive values, the points also increase in curvature (0.310). While also increasing with elevation, lake distance and curvature, the snowpack decreases in depth (-0.427) and temperature at the bottom of the snowpack (-0.326). Higher elevation results in higher ablation to the snow surface, ensuing a lower depth and less snow insulation upon the snowpack bottom, decreasing snowpack temperatures (Zhang, 2005, p.4).

PC2 forms 14.4% of the correlation forcing, where cloud radiative forcing is visible. With cloud cover and temperature top being dominant within this component. Increasing cloud cover at 0.576 and increased curvature or convexity at a lower 0.356 has resulted in an increased surface temperature at 0.613. Serreze and Barry (2014, p.139) and Curry (1996) outline this process.

PC3 represents a relationship between albedo and sine aspect of the slope, which forms 12.5% of the correlation forcing. A value of -0.611 represents a decline in surface albedo as caused by a positive 0.682 value for sine aspect, meaning easterly slopes have a snowpack with reduced albedo. PC4 describes a relationship between density of the snowpack and two Terrain features: curvature and cosine of slope aspect. PC4 forms 11.5% of the correlation forcing. The analysis highlights an increase in ground curvature (0.347) towards a more convex topography alongside an increase northerliness of slope (0.511) decreasing snowpack density (-0.702).

4.5.2 Principal components analysis for all variables (PCA2)

Principal Component Analysis: Temp Bottom, Temp Top, MOD11A2, Density, Albedo, MOD09Q1, MOD09GQ, Depth, Elevation DEM, Curvature, Sine Aspect, Cosine Aspect, Distance from Lake and Cloud Cover

Eigen analysis of the Correlation Matrix
58 cases used, 7 cases contain missing values

Eigenvalue	3.0794	1.8586	1.5399
Proportion	0.220	0.133	0.110
Cumulative	0.220	0.353	0.463

Variable	PC1	PC2	PC3
Temp Bottom	-0.221	0.246	-0.032
Temp Top	-0.114	-0.451	0.204
MOD11A2	-0.321	-0.413	-0.054
Density	0.216	0.025	0.258
Albedo	0.048	0.164	0.484
MOD09Q1	0.340	0.104	-0.007
MOD09GQ	-0.015	-0.115	0.515
Depth	-0.342	0.095	-0.080
Elevation DEM	0.522	0.030	-0.027
Curvature	0.215	-0.403	-0.125
Sine Aspect	-0.016	0.063	-0.376
Cosine Aspect	-0.082	0.046	-0.425
Distance of Lake	0.458	0.018	-0.184
Cloud Cover	0.138	-0.579	-0.097

+ve CosX = Northerliness +ve SinX = Easterliness
-ve CosX = Southerliness -ve SinX = Westerliness

Figure 9: Principal Component Analysis for all MODIS variables. Full PCA in appendix F.2.

This PCA compares the 10 ground variables alongside satellite information for daily and composite albedo (MOD09GQ/Q1) and composite LST (MOD11A2). PCA1 is dominated by five forcing variables at a percentage of 22.0% of the correlation. These include elevation distance from lakes, snow depth, CST and CSA. Topography changes whilst elevation increases (0.522) and distance from the lake increases (0.458), so such do the composite readings for LST and Albedo. LST readings decrease at a value of -0.321 and albedo readings increase at a value of 0.340, while snow depth decreases. Overall, depth of snow and CST are expected to decrease with elevation, which itself increases with distance from the valley lakes. Albedo could be increased alongside elevation due to the sparse shading from vegetation and topography that ensues at the higher elevation sites throughout Kevo. These areas allow for uninterrupted radiation and reflection, giving an albedo value with little interference.

PC2 forms 13.3% of the correlation forcing, and can be explained similarly to PC2 in PCA1. PC2 shows cloud radiative forcing at a manual and satellite scale, but in a negative trend. As cloud cover decreases (-0.579) so does curvature (-0.403) toward concave topography, while alongside these temperatures manually recorded and

recorded by MOD11A2 decrease by -0.451 and -0.413, respectively. This shows that without cloud cover, surface temperature long wave insulation is reduced, leading to decreased temperatures. This trend is also correlated with ground concavity. PC3 forms 11% of the correlation forcing and is explained by DSA (0.515). It is influenced by cosine (-0.425) and sine of the slope aspect (-0.376). These values indicate that south facing and west-facing slopes leads to a higher DSA.

4.6 Summary of analysis

It has been concluded that the use of Terra over Aqua datasets is necessary due to the bias of morning recorded points and that both datasets show similar differences to the manual data—meaning comparisons for each would result in similar conclusions. Findings that CSA and DSA differed in coverage were clear, with cloud contamination evident between albedo and cloud cover. Micro-scale relationships could be derived for elevation and albedo, though there are inconsistencies between all three albedo measurements. Surface temperatures showed evidence of cloud radiative forcing and the inability of satellites to measure such surface temperatures due to cloud cover, which reduced pixel recordings. Both PCAs developed an understanding of the valley variable relationships and often supported previous satellite vs manual maps. Where PC2 of each PCA recognised a form of cloud radiative forcing, while also various PCs describe known and lesser known relationships such as the effect of elevation on snowpack depth and base temperature, and the effect of elevation (PC1 of PCA2) and aspect (PC3 of each PCA) on albedo. Satellite datasets are only as good as the synoptic conditions throughout the week.

Chapter 5:

Discussion

5.0 Discussion

5.1 Synoptic conditions: Resultant radiative forcing

Synoptic conditions provide the prologue for climate and weather for the day, as shown in Figure 10.

Two synoptic charts represent the common low pressure conditions of the study week and one rare

high pressure day. High pressure days as outlined by McIlveen (1992, p.271) are large areas of subsiding, cloud-free air; whereas in low pressure systems air rises and water vapour condenses forming a cloud layer. These processes are shown in the right and left synoptic charts in

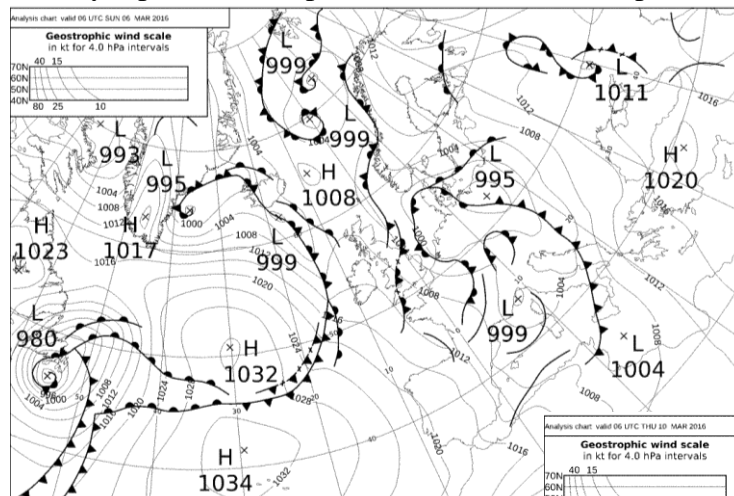


Figure 10. Day 66 is a fair representation of the majority of the week's synopticity until day 70 where a high pressure system was dominant for one full day.

Within the data and the analysis this has resulted in an interesting range across manual and satellite datasets. Disparities between LST datasets from

manual to MOD11A1 and MOD11A2, are due to the aforementioned conditions, and data analyses has highlighted cloud radiative forcing. While this process has been described previously, its Arctic importance has not, this long wave emissivity warming effect, like that of greenhouse gases (Minnett, 1998, p.147) has been summarised by many studies and labelled as the 'largest uncertainty in global climate model projections for future climate change' by Zelinka and Hartmann (2010, p.1). Results from the week dataset are relatively short, as Cogley and Henderson-Sellers' (1984) investigations had similar findings, where positive cloud radiative forcing was evident across snow-covered ground. The IPCC struggles to define the impact of cloud radiative forcing within its fourth assessment report, instead suggesting it is of global significance (Zelinka & Hartmann, 2010, p.1). Therefore, its assessment of importance to global climate forecasting and satellite representability against in situ readings is necessary for reliability.

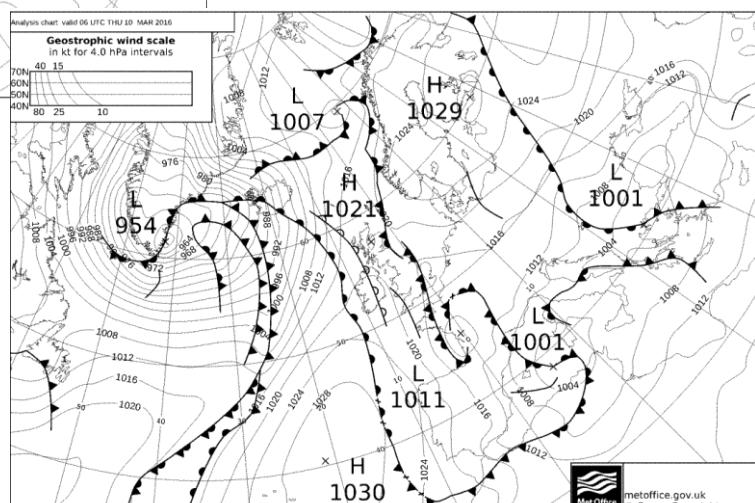


Figure 10: Synoptic charts comparing weather between 6th March (Day 66 – left) and 10th March (Day 70 – right). Retrieved from www.willandweather.org.uk/mycharts.php (2016).

5.2 MODIS representation of cloud cover

For all MODIS sensors, cloud cover removal is within the data collection algorithms. Often it is most accurate where disparities between ground and cloud are large, including variables such as reflectance and temperature. This process is known as the MODIS cloud mask, where several bands are run through the algorithm and classed for either cloud cover or not. However, parts of this process have been described as ‘not advisable’ for situations, including cloud covered snow (Ackerman et al, 1998), which describes the majority of the conditions found across the study week.

Evidence within the analysis of daily MODIS representation of cloud cover shows, firstly, within the LST data where all MOD11A1 daily data (except day 70) shows little to no pixel recordings (Map 11). An algorithm did not remove cloud for these days; the data was just uncollectable. However, MOD09GQ was able to record daily surface reflectance for the week.

Initially this comparison of data collection between both sensors is confusing, as it would be expected that if the cloud mask algorithm was in action, data for cloud covered days would be removed. This leads to the assumption that these daily recordings may well be cloud reflectance. Within a study by Minnett (1998), the values for various satellite data vs ground based recordings range from 5% to 40% for the Arctic, where this difference is gained from a study by Schweiger and Key (1992) for data during cloudier sky days. Furthermore, it is found that satellite measurements find difficulty in distinguishing clouds over a snow/ice-covered surface channel (Li & Leighton, 1991; Schweiger & Key, 1992). This can be believed to be the case for MODISs cloud mask algorithm, with contamination in many studies and only the use of clear sky days possible (Bosilovich, 2006; Comiso, 2003; Crosman & Horel, 2009; Hall et al, 2004). Within recent studies, the cloud mask is believed to not fully remove cloud cover for surface data reliability, and a range of secondary cloud removal methods have been attempted; however, often only satisfactory results can be obtained and this is only for rare occasions (Hu et al, 2015).

5.3 The compromise between field data and satellite data

It is unclear whether MODIS datasets are ever cloud contamination free, but from these findings, the composite datasets attempt to remove cloud cover by extrapolating values for only clear days, given incorrect LST readings, and in the case of the Arctic winter, cloud radiative forcing is a positive forcing factor resulting in disparities. However, with these errors in mind, satellite data is necessary in the Arctic for coverage; in similar remote landscapes, as manual data records would be impossible and meteorological stations are sparse in coverage (Hachem et al, 2012; Comiso, 2003; Crosman & Horel, 2009).

With experiments in the field becoming more expensive, remote sensing from satellite data is increasing in popularity (Bosilovich, 2006, p.1). As a result, further caution must be taken when applying such data. Without consideration of subset layers, such as ‘Quality Control’, false representation is possible. However, it is arguable that data for an area that otherwise may be unmeasurable is better than the unknown, at least to develop difference trends. Satellites also can record, not only the unknown but also areas of large scale, as shown by Coll et al (2005). Where 13 km² of rice crops were analysed for LST from MODIS and AASTR, this study also found that uncertainty is not only among MODIS but also among AASTR where LST was overestimated at 3°C (Coll et al, 2005, p.298) and on clear days MODIS was accurate, as mirrored in Map 13’s micro project for day 70. MODIS accuracy is also further seen in non-Arctic studies such as Reinart and Reinhold (2008, p.610) where in situ measurements were in accordance with sea surface temperatures. Often academics conclude that the only real compromise between satellite and field data for accurate results, is increased in situ ground measurements for further data validation (Coll et al, 2005, p.299; Comiso, 2003, p.3499).

Chapter 6:

Conclusion

6.0 Conclusion

By bringing this study of Kevo Valley variables and its representability on a global satellite scale to an end, it can be said that satellite data is not fully representative of daily Arctic variability and its specific components. This study of in situ manual recordings has highlighted climatic conditions that otherwise would be unclear from a remotely sensed perspective. Evidence of cloud radiative forcing is recognisable between the clear day 70, and the rest of the week. Use of the MODIS sensor has shown that daily LST data (MOD11) is unable to record pixel values for cloud covered ground, and that 8-day composite datasets are often just an average of clear day data across a whole week. In the case of Kevo Valley, this is inappropriate given data that can be as much as 8.14 °C (TSACOL) away from Arctic reality. Conversely, remote sensing offers the ability to assess inaccessible areas of sparse manual data collection such as the Arctic. This ability is both an important opportunity for climatic data in otherwise unknown regions but also must be compared along subsequent synoptic data and satellite quality control datasets, before being further used within global averages. Satellite systems are an ever-developing field that aim to give surface representability, nonetheless currently, manual ground data is invaluable for accurate and true data. Without this, cross comparison between further satellite developments would be impossible, and the Arctic reality could soon become the Arctic unknown.

6.1 Critical reflection

In hindsight, there are parts of the study that, while unavoidable, would now be considered necessary for further study. Synoptic conditions are important for clear satellite conditions, if the subject of interest is a ground variable. With clear sky conditions, such as day 70, a consistent study would have been possible between satellite variables and ground variables, which would have yielded a weeks' worth of MOD11A1 data. Alongside this, during the visit in this particular week in March 2016, there were variable climatic conditions where towards the end of the week, forecast temperatures were above freezing—a rare situation for this location. The ability to carry out research earlier into the winter months may resolve this inconsistent climate.

Lastly, the study may have benefited from a second study week, where I as a researcher would have been experienced in the relevant field methods for accurate data collection; and more results would create larger data to compare and analyse against satellite measurements.

6.2 Further research

This study may be better furthered with the use of Apogee Instruments SI-121: Narrow Field of View Infrared Radiometer Sensor (Apogee Instruments, 2016). It is claimed that typical applications for this instrument includes terrestrial snow layer, and this sensor has an 18° field of view and is often set at an angle to the surface much like figure 11.

Recent data acquisition from March 2017 by Pepin (2017) enabled a small regression to be carried out, for initial comparisons for SI-121 against MODIS MOD11A1. The days available for comparison are shown in table 10, they were – as with previous study – governed by clear sky days resulting in available MODIS data. Both day and night LST recordings have been compared, due to the continuous recordings by SI-121 from the 10th to 22nd March 2017.



Figure 11: SI-121 in the field, photo of clear site experiment. Retrieved from Pepin (2017).

<i>Site</i>	<i>Year</i>	<i>Month</i>	<i>Day</i>	<i>Time</i>	<i>Effective Surface Temperature (°C)</i>	<i>MOD11A1 LST (°C)</i>
<i>Clear</i>	2017	3	10	1135	-15.55	-12.59
<i>Clear</i>	2017	3	10	2120	-19.65	-13.43
<i>Clear</i>	2017	3	12	1135	-7.65	-8.17
<i>Clear</i>	2017	3	12	2105	-6.05	-14.15
<i>Birch</i>	2017	3	14	2050	0.35	-9.73
<i>Birch</i>	2017	3	15	2000	-2.25	-6.75
<i>Birch</i>	2017	3	16	2040	-6.85	-9.77
<i>Birch</i>	2017	3	17	2130	-7.25	-9.57
<i>Pine</i>	2017	3	19	1130	-11.55	-13.47
<i>Pine</i>	2017	3	19	2115	-18.25	-17.31
<i>Pine</i>	2017	3	20	2200	-7.15	-10.93
<i>Pine</i>	2017	3	21	1115	-1.45	-6.37
<i>Pine</i>	2017	3	21	2105	-6.05	-10.11
<i>Pine</i>	2017	3	22	1200	1.55	-2.11

Table 11: Data table for SI-121 sensor vs MOD11A1, 2017 study. Data provided by Pepin (2017).

Further comparison has been carried out for each site and across the overall dataset below in figure 11.

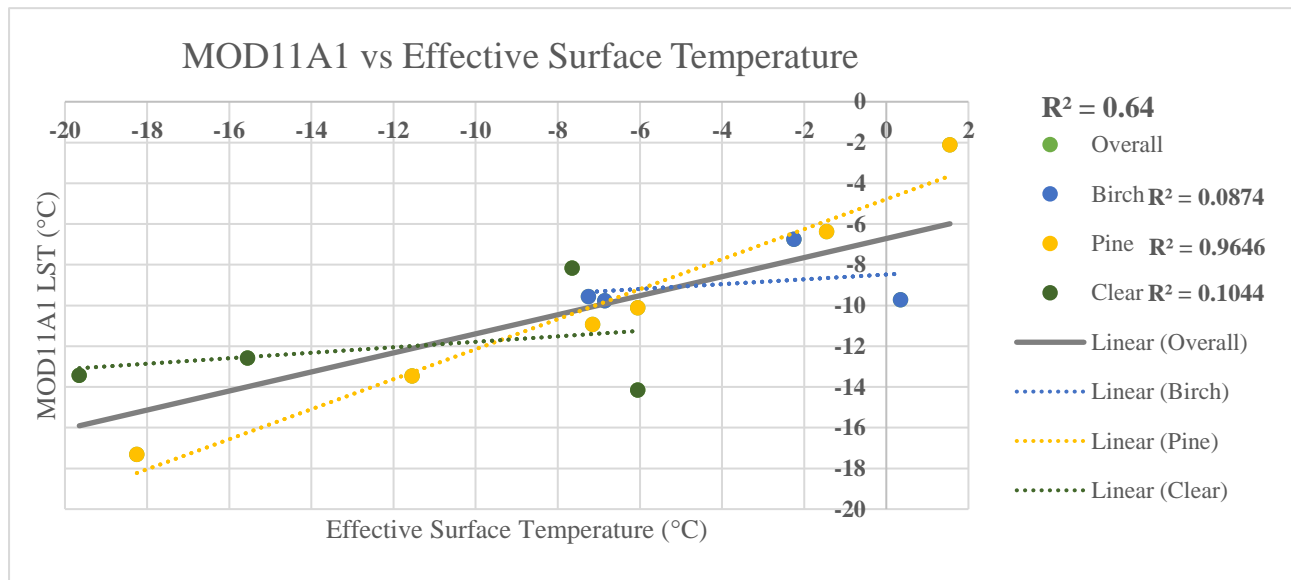


Figure 12: Correlation coefficients for both the overall dataset and the site specific data sets. Data provided by Pepin (2017).

The graph above in figure 12 shows, an overall correlation coefficient of 0.8 across the whole dataset shows a good likeness between the data, however when each site is considered interesting result for both birch site and clear site are found. Where coefficients for each are 0.2956 and 0.3231 respectively. If we lastly consider pine site the strongest correlation is shown between the data at 0.9821. One may expect the strongest relationship to be between clear sites and the MOD11A1 however for this small dataset this is not the case. Conversely, pine site has the strongest relationship with the satellite data which maybe be due to increased results for clear sky satellite days and also the difference being opposite, so as to place the correlation between two values. Lastly, Birch site may not be well represented due to all data being night time data, again due to poor satellite coverage during the day, because of cloud influencing. However, most importantly the overall coefficient of 0.8 is more than 71% stronger than that between the MOD11A2 composite and manual top temperature from this study, at 0.231. It can therefore be considered that this sensor is able to show a closer comparison with satellite data than the previous sensor, with only 22% of the data measurements than the previous sensors dataset. Even at this early stage of analysis results are promising.

Subsequent research has also resulted in interest within two satellite opportunities for further study. Snow Data Assimilation System (SNODAS) Data Products at NSIDC, Version 1 (Qu et al, 2006, p.155; "National Snow and Ice Data Center", n.d.) Where by new products are being recorded, and obtain across northern America for snow datasets. Radarsat-2 Canadian space agency (Serreze and Barry, 2014, p.17) also offers a secondary form of remote sensing across the Arctic's 'cloudy' landscape.

Chapter 7:

References

7.0 References

- ACIA (2005), Arctic Climate Impact Assessment, Cambridge Univ. Press, New York.
- Ackerman, S., Strabala, K., Menzel, W., Frey, R., Moeller, C., & Gumley, L. (1998). Discriminating clear sky from clouds with MODIS. *Journal Of Geophysical Research: Atmospheres*, 103(D24), 32141-32157.
- Arctic Ocean Base. (2015). Arcgis.com. Retrieved 14 March 2017, from <https://www.arcgis.com/home/item.html?id=305cb48615d743f89fe70ff3a819e59e>
- Apogee Instruments. (2016). INFRARED RADIOMETER: Models SI-111, SI-121, SI-131, and SI-1H1. Retrieved from <http://www.apogeeinstruments.co.uk/narrow-field-of-view-infrared-radiometer-sensor-si-121/>.
- ArcGIS Desktop Help 9.3 - curvature. (2011). Webhelp.esri.com. Retrieved 11 March 2017, from <http://webhelp.esri.com/arcgisdesktop/9.3/index.cfm?TopicName=curvature>
- Barrett, E. C., & Curtis, L. F. (1999). An introduction to environmental remote sensing (4th ed.). Cheltenham, Glos., UK: Stanley Thornes Publishers.
- Bernstein, L., Bosch, P., Canziani, O., Chen, Z., Christ, R., & Riahi, K. (2008). IPCC, 2007: climate change 2007: synthesis report. IPCC.
- Bosilovich, M. (2006). A comparison of MODIS land surface temperature with in situ observations. *Geophysical Research Letters*, 33(20).
- Campbell, J. B., & Wynne, R. H. (2011). Introduction to remote sensing (5th ed.). New York: Guilford Publications.
- Chapin, F. S., Sturm, M., Serreze, M. C., McFadden, J. P., Key, J. R., Lloyd, A. H., McGuire, A. D., Rupp, T. S., Lynch, A. H., Schimel, J. P. & Beringer, J. (2005). Role of land-surface changes in Arctic summer warming. *Science*, 310(5748), 657-660.
- Chapin, S. F., Shaver, G. R., & Svoboda, J. (1992). Arctic ecosystems in a changing climate: An ecophysiological perspective. London: Academic Press.
- Coakley, J. (2002). Reflectance and albedo, surface. In J. R. Holton, J. A. Curry, & J. A. Pyle, (Eds.), *Encyclopedia of the Atmospheric Sciences* (pp. 1914 – 1923). Cambridge: Academic Press.
- Cohen, J., Screen, J. A., Furtado, J. C., Barlow, M., Whittleston, D., Coumou, D., ... Jones, J. (2014). Recent arctic amplification and extreme mid-latitude weather. *Nature Geoscience*, 7(9), 627–637.
- Coll, C., Caselles, V., Galve, J., Valor, E., Niclos, R., Sanchez, J., & Rivas, R. (2005). Ground measurements for the validation of land surface temperatures derived from AATSR and MODIS data. *Remote Sensing Of Environment*, 97(3), 288-300.
- Comiso, J. (2003). Warming Trends in the Arctic from Clear Sky Satellite Observations. *Journal Of Climate*, 16(21), 3498-3510.
- Cox, C. (2016). Photograph of Richard overlooking Kevo Lake.

- Crosman, E., & Horel, J. (2009). MODIS-derived surface temperature of the Great Salt Lake. *Remote Sensing Of Environment*, 113(1), 73-81.
- Cubasch, U., & Cess, R. D. (1990). Processes and modelling. *Climate Change: The IPCC Scientific Assessment*, 69-72.
- Curry, J., Schramm, J., Rossow, W., & Randall, D. (1996). Overview of Arctic Cloud and Radiation Characteristics. *Journal Of Climate*, 9(8), 1731-1764.
- Curvature function. (2016). Desktop.arcgis.com. Retrieved 13 March 2017, from <http://desktop.arcgis.com/en/arcmap/10.4/manage-data/raster-and-images/curvature-function.htm>
- DAAC2Disk | LP DAAC :: NASA Land Data Products and Services. (2014). Lpdaac.usgs.gov. Retrieved 12 March 2017, from https://lpdaac.usgs.gov/data_access/daac2disk
- Delta T. (2000). *Energy Sensor ES2 User Manual 1.0*. Retrieved from <http://www.delta-t.co.uk/wp-content/uploads/2016/10/ES2-Energy-Sensor-UM.pdf>
- DeMers, M. (2009). Fundamentals of geographic information systems (4th ed.). Hoboken, NJ: Wiley.
- Donald, J. R., Soulis, E. D., Kouwen, N., & Pietroniro, A. (1995). A land cover-based snow cover representation for distributed Hydrologic models. *Water Resources Research*, 31(4), 995–1009.
- Evans, J. (1996). Straightforward statistics for the behavioral sciences (1st ed.). Pacific Grove: Brooks/Cole Pub. Co.
- Foody, G. M., & Atkinson, P. M. (Eds.). (2002). Uncertainty in remote sensing and GIS. Chichester, West Sussex, England: John Wiley & Sons.
- Grace, J. (2002). Impacts of Climate Change on the Tree Line. *Annals Of Botany*, 90(4), 537-544.
- Hachem, S., Duguay, C., & Allard, M. (2012). Comparison of MODIS-derived land surface temperatures with ground surface and air temperature measurements in continuous permafrost terrain. *The Cryosphere*, 6(1), 51-69.
- Hall, D. K., & Riggs, G. A. (2007). Accuracy assessment of the MODIS snow products. *Hydrological Processes*, 21(12), 1534–1547.
- Hall, D., Key, J., Case, K., Riggs, G., & Cavalieri, D. (2004). Sea ice surface temperature product from MODIS. *IEEE Transactions On Geoscience And Remote Sensing*, 42(5), 1076-1087.
- Hantel, M., Ehrendorfer, M., & Haslinger, A. (2000). Climate sensitivity of snow cover duration in Austria. *International Journal of Climatology*, 20(6), 615–640.
- Heywood, I. D., Cornelius, S., & Carver, S. (2011). An introduction to geographical information systems (4th ed.). Harlow, England: Prentice Hall.
- Hu, Y., Huang, J., Du, Y., Han, P., Wang, J., & Huang, W. (2015). Monitoring wetland vegetation pattern response to water-level change resulting from the Three Gorges Project in the two largest freshwater lakes of China. *Ecological Engineering*, 74, 274-285.
- Indiana University. (2015, July 6). What are GIS and remote sensing? Retrieved February 27, 2017, from Indiana University: Knowledge Base, <https://kb.iu.edu/d/anhs>

- Jenness, J. (2007). Some thoughts on analyzing topographic habitat characteristics. Jenness Enterprises, Flagstaff, AZ, USA, 26.
- Jones, K. (2009). Secondary data analysis. In D. Gregory, *The dictionary of human geography*. Oxford, UK: Blackwell Publishers. Retrieved from http://search.credoreference.com/content/entry/bkhumgeo/secondary_data_analysis/0?institutionId=129
- Li, Z., & Leighton, H. (1991). Scene identification and its effect on cloud radiative forcing in the Arctic. *Journal Of Geophysical Research*, 96(D5), 9175.
- Lillesand, T., Kiefer, R. W., & Chipman, J. (2014). *Remote sensing and image interpretation* (7th ed.). Hoboken, NJ, United States: John Wiley & Sons.
- Lunetta, R. S., Knight, J. F., Ediriwickrema, J., Lyon, J. G., & Worthy, L. D. (2006). Land-cover change detection using multi-temporal MODIS NDVI data. *Remote Sensing of Environment*, 105(2), 142–154.
- McKay, G. A., & Gray, D. M. (1981). The distribution of snowcover. *Handbook of snow*.
- Mirzaei, R. & Sakizadeh, M. (2015). Comparison of interpolation methods for the estimation of groundwater contamination in Andimeshk-Shush Plain, Southwest of Iran. *Environmental Science And Pollution Research*, 23(3), 2758-2769.
- Morain, S. A., & Budge, A. M. (2004). Post-launch calibration of satellite sensors: Proceedings of the international workshop on Radiometric and geometric calibration, December 2003, Mississippi, USA. United Kingdom: CRC Press.
- NASA,. (2005). Sample Aqua Orbital Tracks from 15 February 2005. Retrieved from https://nsidc.org/sites/nsidc.org/files/aqua_tracks.20050215.gif
- NASA,. (2005). Sample Terra Orbital Tracks from 15 February 2005. Retrieved from https://nsidc.org/sites/nsidc.org/files/terra_tracks.20050215.gif
- NASA. (2015, July 31). Terra Spacecraft. Retrieved February 28, 2017, from [www.nasa.gov](https://www.nasa.gov/mission_pages/terra/spacecraft/index.html), https://www.nasa.gov/mission_pages/terra/spacecraft/index.html
- NASA. (2016, December 2). Land Surface Temperature/Emissivity (MOD11). Retrieved March 5, 2017, from [www.modis-land.gsfc.nasa.gov](https://modis-land.gsfc.nasa.gov), <https://modis-land.gsfc.nasa.gov/temp.html>
- National Snow and Ice Data Center. Nsidc.org. Retrieved 17 March 2017, from <http://nsidc.org/data/g02158>
- Ofungwu, J. (2014). *Statistical applications for environmental analysis and risk assessment* (1st ed., p. 438). Hoboken, NJ: Wiley.
- O'Hare, G., & Sweeney, J. (1986). *The atmospheric system* (1st ed., p. 17). Cartermills Publishing.
- Pepin, N. (2017). Meteorological field data, March 2017, University of Portsmouth.
- Pepin, N., Bradley, R. S., Diaz, H. F., Baraer, M., Caceres, E. B., Forsythe, N., ... Yang, D. Q. (2015). Elevation-dependent warming in mountain regions of the world. *Nature Climate Change*, 5(5), 424–430.

- Qu, J., Gao, W., Kafatos, M., Murphy, R., & Salomonson, V. (2006). Earth science satellite remote sensing (1st ed.). Berlin: Springer.
- Rasmus, S. (2005). Snow pack structure characteristics in Finland: Measurements and modelling. Helsinki: University of Helsinki.
- Reese, M. (2016). Near Real-Time Data Frequently Asked Questions - EOSDIS Support Knowledge base - Earthdata Wiki. Wiki.earthdata.nasa.gov. Retrieved 17 March 2017, from <https://wiki.earthdata.nasa.gov/display/ESKB/Near+RealTime+Data+Frequently+Asked+Questions>
- Rhind, D. W., (1989). Why GIS? *ARC News*. (Summer), 28-29.
- Saunders, S., Montgomery, C. H., Easley, T., & Spencer, T. (2008). Hotter and drier: the West's changed climate. Rocky Mountain Climate Organization.
- Schweiger, A., & Key, J. (1992). Arctic Cloudiness. Comparison of ISCCP-C2 and Nimbus-7Satellite-derived Cloud Products with a Surface-based Cloud Climatology. *Journal Of Climate*, 5(12), 1514-1527.
- Serreze, M. C., & Barry, R. G. (2014). The Arctic Climate System. Cambridge: Cambridge University Press (Virtual Publishing).
- STRÅNG data extraction. (2011). Strang.smhi.se. Retrieved 16 March 2017, from <http://strang.smhi.se/extraction/index.php>
- Stroeve, J., Box, J. E., Gao, F., Liang, S., Nolin, A., & Schaaf, C. (2005). Accuracy assessment of the MODIS 16-day albedo product for snow: Comparisons with Greenland in situ measurements. *Remote Sensing of Environment*, 94(1), 46–60.
- Thomas, D. S. G., & Goudie, A. (Eds.). (2000). The dictionary of physical geography (Third Edition ed.).
- Thome, K. J., Czapla-Myers, J. S., & Biggar, S. F. (2003). Vicarious calibration of Aqua and terra MODIS. *Earth Observing Systems VIII*.
- Tree Line. (2015). Arcgis.com. Retrieved 11 March 2017, from <http://www.arcgis.com/home/item.html?id=2d90f663eaee4c7a8310b24e77b29fbe>
- University of Portsmouth. (n.d.) University of Portsmouth Crest. Retrieved from <http://www.port.ac.uk/alumni/>
- Vermote, E. (2015). MODIS Surface Reflectance User's Guide: Collection 6. Retrieved from https://lpdaac.usgs.gov/sites/default/files/public/product_documentation/mod09_user_guide_v1.4.pdf
- Vermote, E. (2015a). MOD09GQ MODIS/Terra Surface Reflectance Daily L2G Global 250m SIN Grid V006. NASA EOSDIS Land Processes DAAC.
- Vermote, E. (2015b). MYD09GQ MODIS/Aqua Surface Reflectance Daily L2G Global 250m SIN Grid V006. NASA EOSDIS Land Processes DAAC.
- Vermote, E. (2015c). MOD09Q1 MODIS/Terra Surface Reflectance 8-Day L3 Global 250m SIN Grid V006. NASA EOSDIS Land Processes DAAC.

- Vermote, E. (2015d). MYD09Q1 MODIS/Aqua Surface Reflectance 8-Day L3 Global 250m SIN Grid V006. NASA EOSDIS Land Processes DAAC.
- Vermote, E. F., El Saleous, N. Z., & Justice, C. O. (2002). Atmospheric correction of MODIS data in the visible to middle infrared: First results. *Remote Sensing of Environment*, 83(1-2), 97–111.
- Wade, T. & Sommer, S. (2006). *A to Z GIS* (1st ed.). Redlands, Calif.: ESRI Press.
- Wan, Z. (1999). MODIS Land-Surface Temperature Algorithm Theoretical Basis Document. Institute for Computational Earth System Science, University of California, Santa Barbara, CA.
- Wan, Z. (2006). MODIS land surface temperature products users' guide. Institute for Computational Earth System Science, University of California, Santa Barbara, CA.
- Wan, Z. (2013). MODIS Land Surface Temperature Products User's Guide: Collection 6. Retrieved from
https://lpdaac.usgs.gov/sites/default/files/public/product_documentation/mod11_user_guide.pdf
- Wan, Z., S. H., G.Hulley. (2015a). MYD11A1 MODIS/Aqua Land Surface Temperature/Emissivity Daily L3 Global 1km SIN Grid V006. NASA EOSDIS Land Processes DAAC.
- Wan, Z., S. H., G.Hulley. (2015b). MOD11A1 MODIS/Terra Land Surface Temperature/Emissivity Daily L3 Global 1km SIN Grid V006. NASA EOSDIS Land Processes DAAC.
- Wan, Z., S. H., Hulley, G. (2015c). MOD11A2 MODIS/Terra Land Surface Temperature/Emissivity 8-Day L3 Global 1km SIN Grid V006. NASA EOSDIS Land Processes DAAC.
- Wan, Z., S. H., Hulley, G. (2015d). MYD11A2 MODIS/Aqua Land Surface Temperature/Emissivity 8-Day L3 Global 1km SIN Grid V006. NASA EOSDIS Land Processes DAAC.
- Wan, Z., Zhang, Y., Zhang, Q., & Li, Z. . (2004). Quality assessment and validation of the MODIS global land surface temperature. *International Journal of Remote Sensing*, 25(1), 261–274.
- Williams, J. (1995). *Geographic information from space: Processing and applications of geocoded satellite images*. Chichester, United Kingdom: J. Wiley, Praxis.
- Williams, M. (2004). Landscapes and water (GEOG 1011): Snow and ice. Retrieved February 3, 2017, from [www.snobear.colorado.edu](http://snobear.colorado.edu/Markw/Intro/Snow/MtnSnowpack/snowpack.html),
<http://snobear.colorado.edu/Markw/Intro/Snow/MtnSnowpack/snowpack.html>
- Wiscombe, W., & Warren, S. (1980). A Model for the Spectral Albedo of Snow. I: Pure Snow. *Journal Of The Atmospheric Sciences*, 37(12), 2712-2733.
- Wolfe, R. E., Nishihama, M., Fleig, A. J., Kuyper, J. A., Roy, D. P., Storey, J. C., & Patt, F. S. (2002). Achieving sub-pixel geolocation accuracy in support of MODIS land science. *Remote Sensing of Environment*, 83(1-2), 31–49.
- Zelinka, M., & Hartmann, D. (2010). Why is longwave cloud feedback positive?. *Journal Of Geophysical Research*, 115(D16).
- Zhang, T. (2005). Influence of the seasonal snow cover on the ground thermal regime: An overview. *Reviews Of Geophysics*, 43(4), 4.

Zhao, M., Heinsch, F. A., Nemani, R. R., & Running, S. W. (2005). Improvements of the MODIS terrestrial gross and net primary production global data set. *Remote Sensing of Environment*, 95(2), 164–176.

Zhao, M., Running, S. W., & Nemani, R. R. (2006). Sensitivity of moderate resolution imaging Spectroradiometer (MODIS) terrestrial primary production to the accuracy of meteorological reanalyses. *Journal of Geophysical Research*, 111(G1),.

Chapter 8:

Appendices

8.0 Appendices

A. Table from (Wan, 2006)

no.	Specification / Action	in V4	in V5
1	clear-sky pixels defined by MODIS cloudmask	at 99% confidence over land at 66% confidence over lakes	at confidence of >= 95% over land <= 2000m at confidence of >= 66% over land > 2000m at confidence of >= 66% over lakes
2	temporal averaging in the 1km LST product (M*D11A1)	yes	no
3	grid size of LST/emissivities in M*D11B1 retrieved from day/night algorithm	5km x 5km (exactly 4.63km)	6km x 6km (exactly 5.56km)
4	number of sub-ranges of zenith view angles	5 for the whole scan swath	2x8 for the whole scan swath
5	effect of topographic slope in the M*D11B1 grid	not considered	considered in the QA
6	option of combined use of Terra and Aqua data in the day/night algorithm	no	yes
7	incorporate the split-window method into the day/night algorithm	partially with initial Ta & cwv, and variables of em31 & em32	fully with em31, em32, Ta and cwv as variables in iterations
8	removing cloud-contaminated LSTs	not implemented	implemented for M*D11A1 and M*D11B1

**B. MODIS Subset tables retrieved from
MOD09GQ and MYD09GQ**

SDS Layer Name	Description	Units	Data Type	Fill Value	Valid Range	Scaling Factor
num_observations	Number of observations per 250m pixel	None	8-bit signed integer	-1	0 to 127	N/A
sur_refl_b01_1	Surface reflectance band 1	Reflectance	16-bit signed integer	-28672	-100 to 16000	0.0001
sur_refl_b02_1	Surface reflectance band 2	Reflectance	16-bit signed integer	-28672	-100 to 16000	0.0001
QC_250m_1	Surface Reflectance 250m Quality Assurance	Bit Field	16-bit signed integer	2995	0 to 4096	N/A
obscov_1	Observation coverage	Percent	8-bit unsigned integer	255	0 to 100	0.01
iobs_res_1	Observation number	None	8-bit unsigned integer	255	0 to 254	N/A
orbit_pnt_1	Orbit pointer	None	8-bit unsigned integer	255	0 to 15	N/A
granule_pnt_1	Granule pointer	None	8-bit unsigned integer	255	0 to 254	N/A

MOD09Q1 and MYD09Q1

SDS Layer Name	Description	Units	Data Type	Fill Value	Valid Range	Scaling Factor
Sur_refl_b01	Surface reflectance band 1	Reflectance	16-bit signed integer	-28672	-100 to 16000	0.0001
Sur_refl_b02	Surface reflectance band 2	Reflectance	16-bit signed integer	-28672	-100 to 16000	0.0001
sur_refl_250m_state_flag	Surface Reflectance 250m State flags	Bit Field	16-bit unsigned integer	65535	0 to 57343	N/A
Sur_refl_qc_250m	Surface Reflectance 250m Band Quality Control flags	Bit Field	16-bit unsigned integer	65535	0 to 32767	N/A

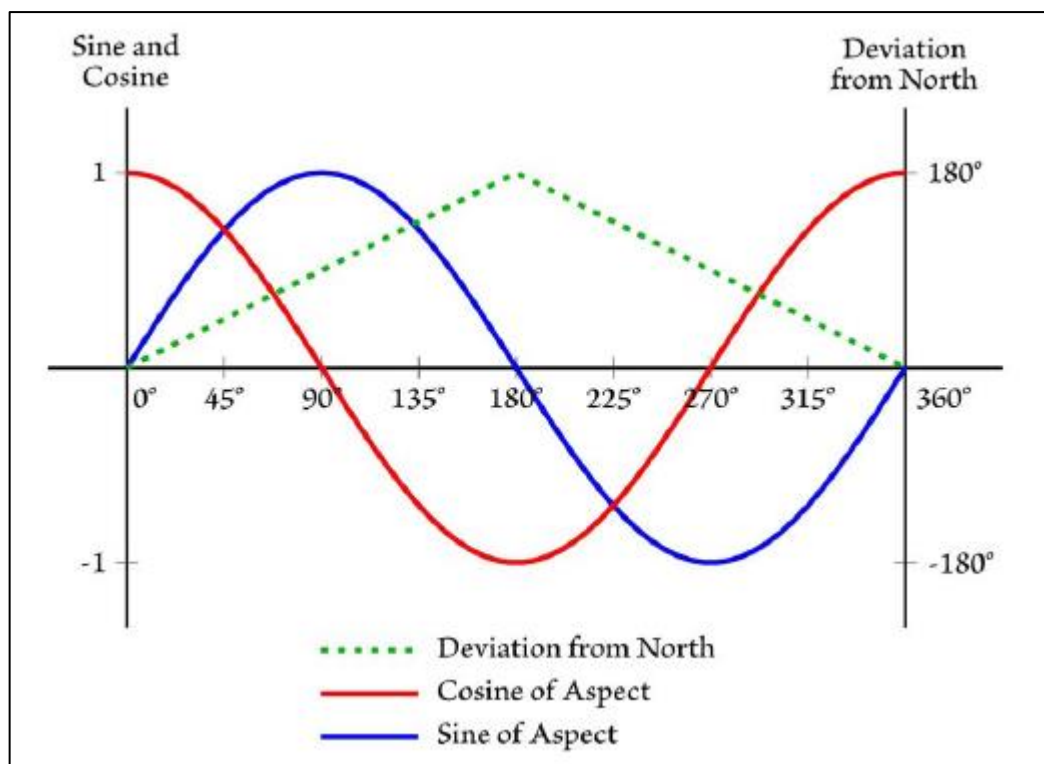
MOD11A1 and MYD11A1

SDS Layer Name	Description	Units	Data Type	Fill Value	Valid Range	Scaling Factor	Additional Offset
LST_Day_1km	Day Land Surface Temperature	Kelvin	16-bit unsigned integer	0	7500 to 65535	0.02	N/A
QC_Day	Daytime LST Quality Indicators	Bit Field	8-bit unsigned integer	N/A	0 to 255	N/A	N/A
Day_view_time	Local time of day observation	Hours	8-bit unsigned integer	255	0 to 240	0.1	N/A
Day_view_angle	View zenith angle of day observation	Degree	8-bit unsigned integer	255	0 to 130	1.0	-65.0
LST_Night_1km	Night Land Surface Temperature	Kelvin	16-bit unsigned integer	0	7500 to 65635	0.02	N/A
QC_Night	Nighttime LST Quality indicators	Bit Field	8-bit unsigned integer	N/A	0 to 255	N/A	N/A
Night_view_time	Local time of night observation	Hours	8-bit unsigned integer	255	0 to 240	0.1	N/A
Night_view_angle	View zenith angle of night observation	Degree	8-bit unsigned integer	255	0 to 130	1.0	-65
Emis_31	Band 31 emissivity	None	8-bit unsigned integer	0	1 to 255	0.002	0.49
Emis_32	Band 32 emissivity	None	8-bit unsigned integer	0	1 to 255	0.002	0.49
Clear_day_cov	N/A	None	16-bit unsigned integer	0	1 to 65535	0.0005	N/A
Clear_night_cov	N/A	None	16-bit unsigned integer	0	1 to 65535	0.0005	N/A

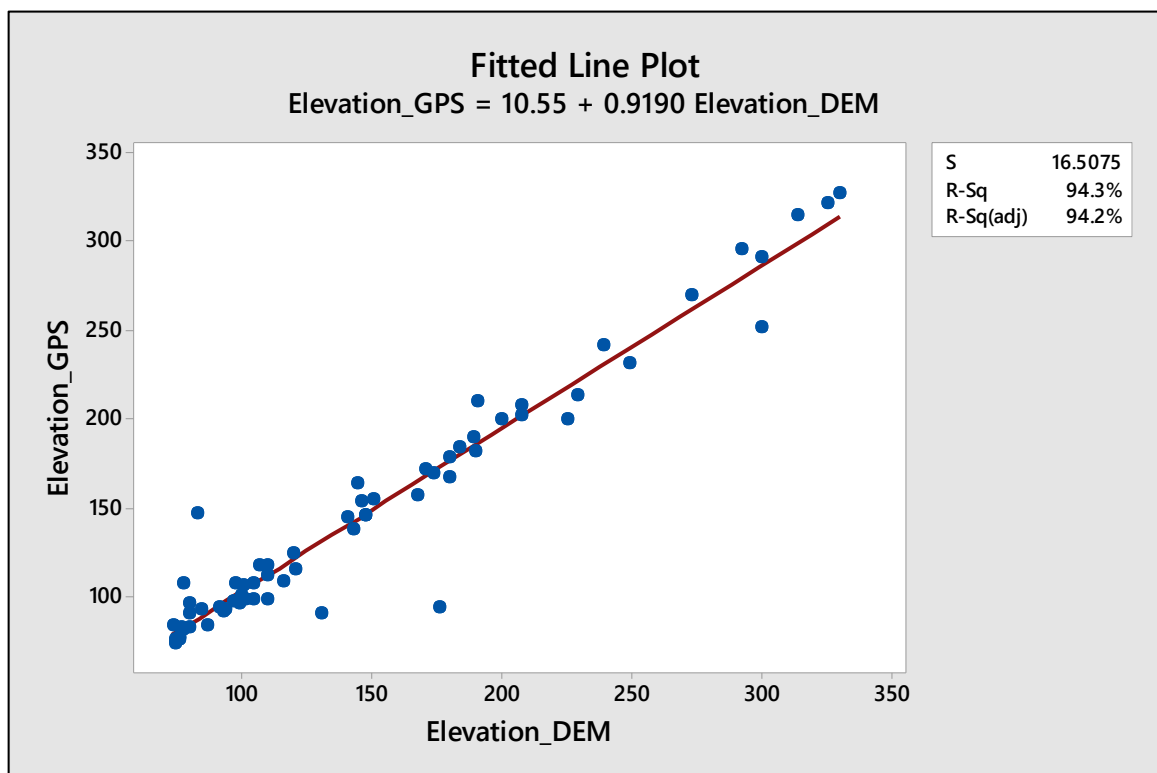
MOD11A2 and MYD11A2

SDS Layer Name	Description	Units	Data Type	Fill Value	Valid Range	Scaling Factor	Additional Offset
LST_Day_1km	Day Land Surface Temperature	Kelvin	16-bit unsigned integer	0	7500 to 65535	0.02	N/A
QC_Day	Daytime LST Quality Indicators	Bit Field	8-bit unsigned integer	N/A	0 to 255	N/A	N/A
Day_view_time	Local time of day observation	Hours	8-bit unsigned integer	255	0 to 240	0.1	N/A
Day_view_angle	View zenith angle of day observation	Degree	8-bit unsigned integer	255	0 to 130	1.0	-65.0
LST_Night_1km	Night Land Surface Temperature	Kelvin	16-bit unsigned integer	0	7500 to 65635	0.02	N/A
QC_Night	Nighttime LST Quality Indicators	Bit Field	8-bit unsigned integer	N/A	0 to 255	N/A	N/A
Night_view_time	Local time of night observation	Hours	8-bit unsigned integer	255	0 to 240	0.1	N/A
Night_view_angle	View zenith angle of night observation	Degree	8-bit unsigned integer	255	0 to 130	1.0	-65
Emis_31	Band 31 emissivity	None	8-bit unsigned integer	0	1 to 255	0.002	0.49
Emis_32	Band 32 emissivity	None	8-bit unsigned integer	0	1 to 255	0.002	0.49
Clear_day_cov	N/A	None	16-bit unsigned integer	0	1 to 65535	0.0005	N/A
Clear_night_cov	N/A	None	16-bit unsigned integer	0	1 to 65535	0.0005	N/A

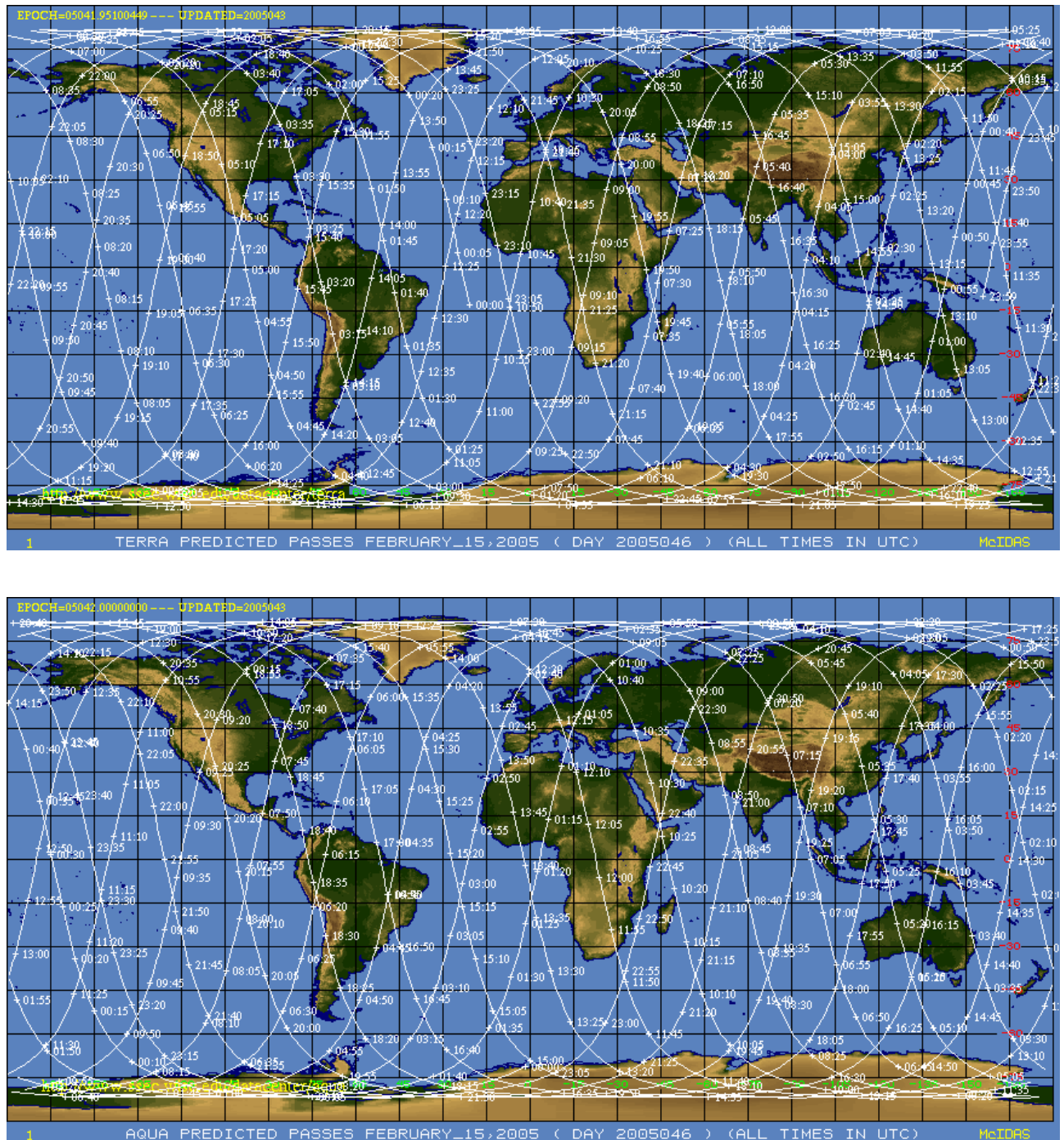
C. Graph from (Jenness, 2007) explaining sine and cosine transformation of aspect degrees.



D. Graph of regression for differing elevations. Performed in Minitab 17.



E. Terra and Aqua path maps (NASA, 2005)



F.1 Principal Component Analysis 1

Principal Component Analysis: Temp Bottom, Temp Top, Density, Albedo, Depth, Elevation DEM, Curvature, Sine Aspect, Cosine Aspect, Distance from Lake and Cloud Cover

Eigenanalysis of the Correlation Matrix
60 cases used, 5 cases contain missing values

Eigenvalue	2.7101	1.5816	1.3700	1.2684	0.9729	0.8521	0.7366	0.4869	0.4441	0.3881
Proportion	0.246	0.144	0.125	0.115	0.088	0.077	0.067	0.044	0.040	0.035
Cumulative	0.246	0.390	0.515	0.630	0.718	0.796	0.863	0.907	0.948	0.983

Eigenvalue	0.1892
Proportion	0.017
Cumulative	1.000

Variable	PC1	PC2	PC3	PC4	PC5	PC6	PC7	PC8	PC9	PC10
Temp Bottom	-0.326	0.092	0.056	-0.177	0.510	-0.545	0.198	-0.453	0.205	0.001
Temp Top	-0.029	0.613	-0.148	-0.206	0.235	0.378	0.039	-0.093	-0.248	-0.533
Density	0.212	0.038	0.242	-0.702	0.144	0.157	-0.104	0.040	-0.224	0.463
Albedo	0.012	-0.227	-0.611	-0.155	0.274	0.208	0.497	0.333	0.244	0.087
Depth	-0.427	0.201	0.034	0.004	0.233	-0.265	-0.278	0.722	-0.132	0.096
Elevation DEM	0.515	-0.148	0.010	-0.057	0.342	-0.145	-0.015	-0.016	-0.115	0.025
Curvature	0.310	0.356	-0.161	0.347	-0.042	-0.348	0.362	0.043	-0.500	0.259
SinAspect	-0.021	-0.052	0.682	-0.006	-0.014	0.074	0.638	0.271	0.032	-0.208
CosAspect	-0.127	-0.116	0.183	0.511	0.563	0.480	-0.088	-0.133	-0.132	0.277
Distance from Lake	0.467	-0.158	0.085	0.089	0.315	-0.196	-0.278	0.232	0.140	-0.458
Cloud Cover	0.264	0.576	0.104	0.129	-0.002	0.077	-0.038	0.079	0.684	0.296

Variable	PC11
Temp Bottom	-0.085
Temp Top	0.072
Density	-0.282
Albedo	-0.091
Depth	0.162
Elevation DEM	0.747
Curvature	-0.241
SinAspect	0.046
CosAspect	-0.097
Distance from Lake	-0.493
Cloud Cover	0.052

F.2 Principal Component Analysis 2

Principal Component Analysis: Temp Bottom, Temp Top, MOD11A2, Density, Albedo, MOD09Q1, MOD09GQ, Depth, Elevation DEM, Curvature, Sine Aspect, Cosine Aspect, Distance from Lake and Cloud Cover

Eigenanalysis of the Correlation Matrix

58 cases used, 7 cases contain missing values

Eigenvalue	3.0794	1.8586	1.5399	1.3884	1.2723	0.9732	0.7846	0.7378	0.5791	0.4884
------------	--------	--------	--------	--------	--------	--------	--------	--------	--------	--------

Proportion	0.220	0.133	0.110	0.099	0.091	0.070	0.056	0.053	0.041	0.035
------------	-------	-------	-------	-------	-------	-------	-------	-------	-------	-------

Cumulative	0.220	0.353	0.463	0.562	0.653	0.722	0.778	0.831	0.872	0.907
------------	-------	-------	-------	-------	-------	-------	-------	-------	-------	-------

Eigenvalue	0.4239	0.3710	0.3361	0.1673
------------	--------	--------	--------	--------

Proportion	0.030	0.027	0.024	0.012
------------	-------	-------	-------	-------

Cumulative	0.938	0.964	0.988	1.000
------------	-------	-------	-------	-------

Variable	PC1	PC2	PC3	PC4	PC5	PC6	PC7	PC8	PC9
----------	-----	-----	-----	-----	-----	-----	-----	-----	-----

Temp Bottom	-0.221	0.246	-0.032	0.374	-0.421	-0.067	-0.041	-0.358	0.328
-------------	--------	-------	--------	-------	--------	--------	--------	--------	-------

Temp Top	-0.114	-0.451	0.204	0.282	-0.242	-0.325	0.272	0.052	-0.286
----------	--------	--------	-------	-------	--------	--------	-------	-------	--------

MOD11A2	-0.321	-0.413	-0.054	-0.187	0.246	-0.163	-0.066	0.069	-0.091
---------	--------	--------	--------	--------	-------	--------	--------	-------	--------

Density	0.216	0.025	0.258	0.560	0.242	-0.109	0.325	0.167	-0.051
---------	-------	-------	-------	-------	-------	--------	-------	-------	--------

Albedo	0.048	0.164	0.484	-0.339	-0.219	-0.175	0.325	-0.418	-0.248
--------	-------	-------	-------	--------	--------	--------	-------	--------	--------

MOD09Q1	0.340	0.104	-0.007	0.103	-0.039	-0.366	-0.614	0.086	-0.474
---------	-------	-------	--------	-------	--------	--------	--------	-------	--------

MOD09GQ	-0.015	-0.115	0.515	-0.025	0.363	-0.236	-0.407	-0.321	0.423
---------	--------	--------	-------	--------	-------	--------	--------	--------	-------

Depth	-0.342	0.095	-0.080	0.278	-0.340	-0.191	-0.278	0.066	0.005
-------	--------	-------	--------	-------	--------	--------	--------	-------	-------

Elevation DEM	0.522	0.030	-0.027	0.018	-0.094	-0.125	0.065	-0.053	0.082
---------------	-------	-------	--------	-------	--------	--------	-------	--------	-------

Curvature	0.215	-0.403	-0.125	-0.129	-0.341	0.274	-0.158	-0.392	-0.167
-----------	-------	--------	--------	--------	--------	-------	--------	--------	--------

Sine Aspect	-0.016	0.063	-0.376	0.323	0.457	0.053	0.080	-0.613	-0.273
-------------	--------	-------	--------	-------	-------	-------	-------	--------	--------

Cosine Aspect	-0.082	0.046	-0.425	-0.276	0.040	-0.694	0.211	-0.082	0.120
---------------	--------	-------	--------	--------	-------	--------	-------	--------	-------

Distance of Lake	0.458	0.018	-0.184	-0.029	-0.084	-0.140	0.092	0.056	0.350
------------------	-------	-------	--------	--------	--------	--------	-------	-------	-------

Cloud Cover	0.138	-0.579	-0.097	0.173	-0.070	-0.015	-0.010	-0.065	0.297
-------------	-------	--------	--------	-------	--------	--------	--------	--------	-------

Variable	PC10	PC11	PC12	PC13	PC14
----------	------	------	------	------	------

Temp Bottom	0.504	-0.182	-0.034	0.204	0.012
-------------	-------	--------	--------	-------	-------

Temp Top	0.074	0.046	-0.498	-0.286	-0.057
----------	-------	-------	--------	--------	--------

MOD11A2	0.131	-0.162	-0.066	0.722	-0.127
---------	-------	--------	--------	-------	--------

Density	0.051	0.293	0.361	0.305	0.233
---------	-------	-------	-------	-------	-------

Albedo	-0.242	-0.280	0.188	0.148	0.076
--------	--------	--------	-------	-------	-------

MOD09Q1	0.177	-0.241	0.080	-0.009	0.149
---------	-------	--------	-------	--------	-------

MOD09GQ	-0.040	0.229	-0.131	-0.123	0.004
---------	--------	-------	--------	--------	-------

Depth	-0.685	0.193	0.093	0.165	-0.120
-------	--------	-------	-------	-------	--------

Elevation DEM	0.012	0.111	-0.023	0.156	-0.806
---------------	-------	-------	--------	-------	--------

Curvature	0.076	0.524	0.095	0.153	0.219
-----------	-------	-------	-------	-------	-------

Sine Aspect	-0.198	-0.115	-0.155	-0.041	-0.053
-------------	--------	--------	--------	--------	--------

Cosine Aspect	0.120	0.275	0.243	-0.163	0.095
---------------	-------	-------	-------	--------	-------

Distance of Lake	-0.279	-0.152	-0.490	0.282	0.417
------------------	--------	--------	--------	-------	-------

Cloud Cover	-0.150	-0.477	0.465	-0.207	-0.002
-------------	--------	--------	-------	--------	--------

G. Raw field data

	A	B	C	D	E	F	G	H	I	J	K	L	M	N	O	P	Q	R	S	T	U	V	W	X	Y	Z	AA	AB	AC	
1	Point	Dateday	Time	Temp_Bottom	Temp_Top	Weight	Density	Ref_In	Ref_Out	Albedo	Depth_Point	Depth_N	Depth_NE	Depth_SE	Depth_SW	Depth_NW	Veg_P	Veg_B	Veg_BS	Veg_PS	Veg_BP	Eastings	Northings	Elevation_GPS	Elevation DEM	Projection				
2	ALLLK	12/03/2016	12:40:00	-11	-3	380	0.348	28	23	0.82	45	50	54	57	53	49	49	41	49	0	4	3	0	0	3500342.92	7742837.47	76	76 KKJ		
3	ALLSUM	12/03/2016	13:10:00	-0.9	-2.5	368	0.3	36	25	0.69	37	56	53	37	41	48	44	46	52	0	5	0	0	0	3500392.82	7742831.9	100	100 KKJ		
4	JE 00	1/1/2016	12:20:00	-5	-7	399	0.424	44	41	0.93	0	7	13	20	15	20	11	11	8	0	0	5	0	0	0	3498360.47	7743563.3	327	330 KKJ	
5	JE E01	1/1/2016	09:43:00	0	-11.5	370	0.308	26	16	0.62	66.5	55	50	37	40	39	67	77	0	8	5	0	0	0	3500015.93	7742391.24	76	75 KKJ		
6	JE E02	06/03/2016	09:55:00	-3	-3.5	348	0.22	31	16	0.52	46.5	49.5	42	48	42	43.5	42	40	46	4	3	0	0	0	3498318.3	7742460.05	84	87 KKJ		
7	JE E03	06/03/2016	10:35:00	-2.5	-3.5	378	0.34	18	12	0.67	47.5	50.5	59	50	51	52	58	50	50	2	2	0	0	0	3498567.91	7742519.6	97	97 KKJ		
8	JE E04	06/03/2016	11:00:00	-0.9	-4	301	0.352	21	10	0.48	60	68.5	63.5	56.5	62	57.5	70	57	65	4	5	0	0	0	3493233.79	7742793.23	144	141 KKJ		
9	JE E05	06/03/2016	11:30:00	-2.1	-5	392	0.396	18	19	1.06	66	70	68	65	61	67	66	66	61	3	5	0	0	0	3490563.73	7742822.86	167	180 KKJ		
10	JE E06	06/03/2016	12:00:00	-0.8	-4	380	0.348	35	16	0.46	50	58.2	44	52	48.6	38.5	58.3	61.5	50	10	4	0	0	0	3498903.97	7743202.23	200	225 KKJ		
11	JE E07	06/03/2016	12:45:00	-2.8	-4	387	0.376	62	42	0.68	17	21	22	18	16	31	20	22	0	0	7	0	0	0	3498653.91	7743620.73	270	273 KKJ		
12	JE E08	06/03/2016	13:30:00	-3.9	-8.5	395	0.408	40	30	0.75	24	36.5	32.2	29.8	26	16	52.3	33.6	30	0	0	4	0	0	0	3498462.93	7743765.89	314	314 KKJ	
13	JE S00	1/1/2016	15:17:00	-0.1	-6	373	0.32	20	16	0.8	59.6	62	66	56.5	60	53	52	55	63	3	6	0	0	0	3498914.52	7742398.99	98	105 KKJ		
14	JE S01	1/1/2016	14:45:00	0.2	-5.5	362	0.276	26	20	0.77	66	63	62.5	65	64	63.5	52.5	68.5	62	0	5	0	0	0	3498756.88	7742586.88	178	180 KKJ		
15	JE S02	1/1/2016	14:10:00	-2.5	-6	361	0.272	54	31	0.57	54	70	72.5	95	61	70	79	67.7	85.5	0	5	0	0	0	0	3498574.84	7742763.63	231	249 KKJ	
16	JES N	06/03/2016	14:25:00	-2.9	-1	402	0.436	45	29	0.64	123.4	95	96	109.6	78.7	43	33	77	54	0	1	0	0	0	0	3498634.73	7744076.47	291	300 KKJ	
17	JETTY	06/03/2016	16:55:00	-2	-3.5	391	0.392	66	38	0.58	51	54	45	54	53.5	54.5	53	65	57.5	0	15	0	0	0	0	3500536.76	7742108.64	83	77 KKJ	
18	JUMB1	12/03/2016	12:20:00	-1.5	-3.5	369	0.304	20	17	0.85	56.5	50	53	56.5	57	54	48	58	52	1	8	0	0	0	0	3500293.93	7743164.71	96	80 KKJ	
19	JUMB2	12/03/2016	12:00:00	-0.7	-1.5	357	0.256	25	17	0.68	68	57	67	68	58	57	59	64	65	4	4	0	0	0	0	3500259.88	7743155.41	91	93 KKJ	
20	KEVH1	09/03/2016	12:30:00	-1.2	-1.5	378	0.34	51	27	0.53	47.5	58.8	55	53	67	77	64	62	57.5	10	1	0	0	0	0	3498912.93	7743947.29	107	98 KKJ	
21	KEVH1	09/03/2016	13:15:00	-0.5	-1.5	394	0.404	28	20	0.71	44.5	55.8	57.7	62	61	59	52	62.2	55.5	1	5	1	0	0	0	3499300.98	7739567.08	93	85 KKJ	
22	KEVY2	09/03/2016	13:50:00	-0.4	-1.5	376	0.332	18	20	1.11	51	54.5	53	49	50.7	57.7	56	48.5	54.3	6	4	0	0	0	0	0	3492993.88	7739885.03	107	105 KKJ
23	KDA1	07/03/2016	14:30:00	-3	-3.5	367	0.296	16	9	0.56	55	66	54	56	60	60	68	55	78	0	10	0	0	0	0	0	3499666.78	7742186.85	98	102 KKJ
24	KDA2	07/03/2016	13:55:00	-2	-4	373	0.32	16	14	0.88	49	64	55	58	58	49	61	62	60	1	3	0	0	0	0	0	3498763.99	7741022.8	153	146 KKJ
25	KPA1	12/03/2016	12:00:00	-1.5	-4	356	0.252	21	15	0.71	51	56	53	51	53	52	55	58	56	0	12	2	0	0	0	0	3500176.22	7743670.44	91	78 KKJ
26	KPA2	12/03/2016	11:05:00	-1.7	-4	312	0.076	27	20	0.74	54	62	49.5	52	48	60	50	52.5	64	11	2	0	0	0	0	1	3500102.87	7743657.43	96	99 KKJ
27	LASSE1	12/03/2016	14:25:00	0	-1.5	359	0.264	12	8	0.67	50.5	51	54	55	55	54	52	52	55	1	1	0	0	0	0	2	3500843.7	7742679.52	112	110 KKJ
28	LASSE2	12/03/2016	14:50:00	-1.3	-3	377	0.336	18	12	0.67	28	37	46	47	37	41	40	31	24	27	5	1	0	0	0	1	3501090.89	7742623.82	138	143 KKJ
29	LASSE3	12/03/2016	15:15:00	-0.2	-1.5	367	0.296	22	21	0.95	55	57	53	49	55	59	61	64	63	3	8	0	0	0	0	0	3501383.76	7742631.39	210	191 KKJ
30	LONE P	1/1/2016	12:41:00	-0.38	-6.5	367	0.296	49	32	0.65	15	20.8	24	29	29.5	28	24	30.5	34.5	1	0	2	0	0	0	0	3498127.36	7743334.79	251	300 KKJ
31	MARTE	10/03/2016	16:14:00	-0.3	0.5	373	0.32	24	16	0.67	56	55	53	59	55.5	62	67	56	56	0	7	0	0	0	0	0	3500933.93	7741618	82	80 KKJ
32	MARTW	10/03/2016	15:48:00	0	-6.5	373	0.32	16	11	0.69	50.5	53	56	57	58.3	65	56.7	57	52	2	1	5	0	0	0	0	3500511.76	7741361.19	73	75 KKJ
33	PUKE1	10/03/2016	11:17:00	-0.1	-6.5	372	0.316	57	46	0.81	50	60	70	69.5	63.2	58	56	58	59	0	10	0	0	0	0	0	3501553.92	7738950.04	118	107 KKJ
34	PUKE2	10/03/2016	11:42:00	0.3	-6	363	0.28	148	153	1.03	63	71	63	67.5	71.5	58	67	66	75	3	7	0	0	0	0	0	3501908.33	7739162.23	169	174 KKJ
35	PUKS1	07/03/2016	09:50:00	-2.6	-3.5	381	0.352	15	12	0.8	47	52	54.5	64	52	59	55	61	58	1	3	0	0	0	0	0	3500354.94	7741974.75	84	74 KKJ
36	PUKS2	07/03/2016	10:00:00	-2.9	-4	392	0.396	21	11	0.52	60.5	57.5	64	65	68	62	73	62	60	1	8	0	0	0	0	0	3500216.85	7741950.57	147	83 KKJ
37	PUKS3	07/03/2016	10:15:00	-2.4	-3	382	0.356	18	14	0.78	42	50	50	56	51	46	36	40	40	10	5	0	0	0	0	0	3500315.94	7741905.95	94	92 KKJ
38	PUKS4	07/03/2016	10:40:00	-0.8	-3	391	0.392	30	21	0.7	68	61	58	60	65	68	70	67	58	0	13	0	0	0	0	0	3500160.77	7741701.42	124	120 KKJ
39	PUKS5	07/03/2016	11:00:00	-1.5	-4	405	0.448	27	15	0.56	36	45	51	50	50	42	36	38	39	1	7	0	0	0	0	0	3500121.23	7741535.94	171	171 KKJ
40	PUKS6	07/03/2016	11:30:00	-2	-3	415	0.488	33	22	0.67	43	55	52	52	61.4	55	54.8	49	58	10	4	0	0	0	0	0	3500040.98	7741443.26	184	184 KKJ
41	PUKS7	07/03/2016	12:00:00	-2	-3.5	373	0.32	40	27	0.68	50	65	62	66	65	60	62	62	67	2	13	0	0	0	0	0	3500057.72	7741444.43	189	189 KKJ
42	PUKSUM	07/03/2016	13:00:00	-3	-4	369	0.304	34	24	0.71	57	75.5	67	68.5	60	67.5	65.5	65	72.3	0	5	0	0	0	0	0	3500040.94	7740663.5	200	200 KKJ
43	PUKV1	10/03/20																												

DEPARTMENT OF GEOGRAPHY

Independent Study Progress Report: Level 6

Answer all of the following questions in the grey boxes. The boxes will expand automatically as you type, however the total document must not exceed 6 sides. See guidance notes on Moodle.

1. PERSONAL DETAILS

First Name(s):	Richard
Last Name:	Hargreaves
Student No:	733160
Degree Programme:	BSc (Hons) Geography
Supervisor:	Dr. Nick Pepin

2. TITLE OF INDEPENDENT STUDY

Enter the provisional title for your dissertation.

A spatial analysis of snow properties across the Kevo Valley System, Finland.

3. AIMS AND OBJECTIVES

Describe the overall aim and list the detailed objectives of your research in order of priority. Objectives should be numbered (300 words).

To create detailed models of the valley snow properties, using terrain analysis for the comparison of the following explanatory variables:

1. Point concavity and convexity
2. Elevation
3. Gradient
4. Distance from lake side
5. Variability of vegetation
6. Direction of slope

To compare models to the statistical analysis such as regression and un-paired T tests

To compare my models for the data collection week with the appropriate MODIS satellite imagery.

To compare the models to atmospheric data across a temporal scale the intention is to analyse the impact of polar warming with climate change.

4. PUBLICATIONS

Using the APA system, list at least 5 publications (i.e. academic journal articles and texts, historical documents, official reports, data sources) that you have read in detail and have led to the identification of these objectives. For each reference give a summary of the salient points in relation to your topic (approx 50 words each).

Pepin, N., Maeda, E., & Williams, R. (2016). Use of remotely sensed land surface temperature as a proxy for air temperatures at high elevations: Findings from a 5000m elevational transect across Kilimanjaro. *Journal Of Geophysical Research: Atmospheres*, 121(17), 9998-10,015.

The research article discusses the comparison of MODIS Land Surface Temperatures to Field point air temperature data, and whether satellite data can give an as reliable and representative data set than the field point data. The data transect is of both the NE and SW slopes across Kilimanjaro. It is found that at lower elevations, satellites are able to give data in correlation to field data however with changing environment they struggle to be consistent. Within the higher elevation alpine and desert regions of Kilimanjaro NE slope, data is widely different from that of the field point. Which is likely explained due to direct radiation to the ground which enables extreme ground heating compared to that of the field air temperature results. A conversion of LST data is then explored using both MODIS NDVI and field point relative humidity. My studies will hope to directly compare MODIS data of both snow properties and temperature over my collection week and time before that over the snow accumulation season. It will be interesting to see how field data can compare to satellite recording here.

Bl, G. & Kirnbauer, R. (1992). An analysis of snow cover patterns in a small alpine catchment. *Hydrol. Process.*, 6(1), 99-109.

The paper gives an introduction into snow runoff and snow cover over a basin in the Austrian alps. As well as recorded data for run off, Bl and Kirnbauer wanted to show the relationship with actual snow properties as taken from satellite data and aerial photography. They describe limitations due to cloud cover and resolution in high elevation regions. The paper gives an example of snow melt modeling from snow cover models mapped to show the change due to terrain features of the area. The focus here is on aerial photography and satellite data, not field data and satellite data this therefore could show interesting comparison to my own study.

Dankers, R. & Christensen, O. (2005). Climate Change Impact on Snow Coverage, Evaporation and River Discharge in the Sub-Arctic Tana Basin, Northern Fennoscandia. *Climatic Change*, 69(2-3), 367-392. This paper firstly discusses an area in northern Fennoscandia, which is close to the study area I am investigating, and in summary looks to show how differing climate scenarios will impact a basins river discharge but also the winter snow period. It shows relevance to the idea of warming enhancement in the Polar Regions and gives possible predictions ideas while also discussing methods of snow loss with increased climate.

Rittger, K., Painter, T., & Dozier, J. (2013). Assessment of methods for mapping snow cover from MODIS. *Advances In Water Resources*, 51, 367-380.

The article outlines key methods for snow cover mapping, with a focus on satellite imagery from MODIS. It gives a strong background on information that can be expected from the variety of imaging available while also evaluating the success of the imagery for truly representing snow cover of an area. While it may not be specific to the northern Finland region, it raises ideas such as NDSI, and gives an idea of images I can expect to find. The evaluation of the satellites relatability will aid with judgement with my own MODIS findings vs my field data.

Lapena, D. & Martz, L. (1996). An investigation of the spatial association between snow depth and topography in a Prairie agricultural landscape using digital terrain analysis. *Journal Of Hydrology*, 184(3-4), 277-298.

The area of focus here is an agricultural site in the Canadian prairies of a much small scale than kevo valley, however the article features use of DEM for assistants in snow cover depth readings and how they may change with topography. Snow depth was recorded similar to my own study. The statistical analysis undertaken reflects what I hope to achieve with the various snow properties correlated to a terrain feature.

5. RESEARCH DESIGN

Describe your overall research design and the theoretical reasons behind your choice of approach (200 words).

The approach to the topic was to undergo primary fieldwork in order to collect actual data rather than relying directly on secondary sources such as MODIS. Prior to the field trip, pure satellite data usage was considered however the ability to collect any physical snow properties would have been impossible without being there. The possibility of lab work to examine snow instead of field collection would have been difficult because of the likely hood of snow melt, as it would not be in its natural environment. Actual field collection up holds the philosophy of science, which is to say that, I can be fully confident that field readings are truth, as long as my human error is null.

6. SPECIFIC METHODS

For each of the numbered objectives listed in Q3, what specific methods are you using to achieve these objectives? (300 words).

Methods of data collection included two temperature probes both manual (for surface temperature) and electronic (for bottom of snowpack/ground temperature). The use of a solarimeter to record reflectance in and out needed for albedo calculation. A Yardstick for depth collection and snow wedge to give weight within a volume for density collection. Both scale and compass are used in combination for snow weight and depth respectively.

Bottom of snow pack temperature collection require no disturbance to the snow other than at the point of collection, a walking pole was used to drive the electronic probe into the snow at one point and enable reliable measurements.

7. INFORMATION COLLECTED

To what extent have you located and/or obtained the information (e.g. data) necessary to meet your research objectives? YOU MUST BE SPECIFIC HERE (300 words).

Field work data collection carried out March 2016, where by I visited all of my interest points across the valley system in relation Dr. Pepin's sites. Here collection of snow depth around the point and at the point was collected as well as snow depth, snow albedo, bottom and top temperature of snow pack and tree type density. This was all primary data collection.

Snow water equivalent calculations are also possible by using snow depth and density data recorded and calculated.

The only secondary data currently collected is 10k resolution MODIS satellite imagery however this is not fine enough and I intend to collect 1k resolution images.

Statistical figures will be collected using SPSS.

8. ANALYSES

How do you intend to analyse/synthesise the information/data you have described in the above section? Specific details of statistical or qualitative techniques are required (300 words).

Statistical analysis will consist of regressions and chi squared mainly for categorical variables, while continuous variables will be analysed using un-paired T tests to show if the two variables correlate or not. Two tests I will undertake are point properties against lake side and not lake side and also point properties above 200m elevation and below 200m elevation.

When comparing more than two variables I will analyse variance. Depth of snow around the compass direction can be analysed in combination with both location and elevations, and the nature of that elevation(hill) use of F tests will be required.

Snow water equivalent may also be useful when considering future warming in the arctic region.

As well as statistical analysis, spatial analysis using various GIS programs will be crucial to the end result of my study. I intend to use isotherm overlay for temperature both bottom and top. While also using the DEM for location variables such as aspect and concavity/convexity. From the DEM and my data I can use terrain analysis tool to give me mappings for properties against topography. These results can then be compared to relevant MODIS data for a comparison of homogeneity.

9. TIMETABLE

Give a DETAILED timetable of future work, with a weekly breakdown for the rest of the academic year (200 words). Please include key milestones.

W/B 14th November: Fully obtained MODIS satellite data of 5k resolution & Begin terrain analysis on QGIS/ArcMap

W/B 21st November: Continue terrain analysis

W/B 28th November: Statistical analysis

W/B 5th December: Statistical analysis

W/B 12th December: Data analysis

W/B 19th December: Data analysis

W/B 26th December: Data analysis
W/B 2nd January: Methodology
W/B 9th January: Literature review
W/B 16th January: Literature review
W/B 23rd January: Review data analysis
W/B 30th January: Introduction and methodology finish
W/B 6th February: introduction and methodology finish
W/B 13th February: Final map processing
W/B 20th February: Review data analysis
W/B 27th February: Conclusion
W/B 6th March: Conclusion
W/B 13th March: Final review and binding
W/B 20th March: Final review and binding
W/B 27th March: Hand in

10. PROBLEMS

If you have run into difficulties, please outline them below and any plans you have for overcoming them (200 words).

Collection of satellite imagery has been difficult to obtain to the correct resolution and in the correct map projection and therefore co-ordinate system. The intention is to use either an imagery projection converter as provided by USGS to convert MODIS imagery to WGS 84. The amount of literature for specifically snow properties in my chosen arctic region has been limited however there is related literature for other areas of polar regions that give substantial information of the relationship between snow properties and other variables such as topography.

11. CONSULTATION

Please outline the extent to which you have consulted with:

- your supervisor, listing personal meetings and other communications;
- relevant external contacts (if applicable).

Dr. Nick Pepin, multiple meetings before summer, with one group meeting on return and my most recent one to one meeting on 13th October.

12. ADDITIONAL REFERENCES

Please list at least 5 additional references relevant to your research. These are NOT to be the same as those reviewed earlier.

- Athick, A. & Naqvi, H. (2016). A method for compositing MODIS images to remove cloud cover over Himalayas for snow cover mapping. 2016 IEEE International Geoscience And Remote Sensing Symposium (IGARSS). <http://dx.doi.org/10.1109/igarss.2016.7730279>
- Dozier, J. & Painter, T. (2004). MULTISPECTRAL AND HYPERSPECTRAL REMOTE SENSING OF ALPINE SNOW PROPERTIES. *Annu. Rev. Earth Planet. Sci.*, 32(1), 465-494.
- Erickson, T., Williams, M., & Winstral, A. (2005). Persistence of topographic controls on the spatial distribution of snow in rugged mountain terrain, Colorado, United States. *Water Resources Research*, 41(4).
- Jost, G., Weiler, M., Gluns, D., & Alila, Y. (2007). The influence of forest and topography on snow accumulation and melt at the watershed-scale. *Journal Of Hydrology*, 347(1-2), 101-115.
- Kour, R., Patel, N., & Krishna, A. (2016). Effects of terrain attributes on snow-cover dynamics in parts of Chenab basin, western Himalayas. *Hydrological Sciences Journal*, 1-16.

13. ETHICS

Have you considered the ethics associated with this research? If you have not already done so, please complete an ethics form and hand in to the Geography Department office.

Yes

14. OTHER INFORMATION

Any other information you wish to add, please do so below.